Article

Really Onychocellids? Revisions and New Findings Increase the Astonishing Bryozoan Diversity of the Mediterranean Sea

Antonietta Rosso [1,2], **Vasilis Gerovasileiou [3]** and **Emanuela Di Martino [4,*]**

1   Dipartimento di Scienze Biologiche, Geologiche e Ambientali, Università di Catania, Corso Italia 57, 95129 Catania, Italy; rosso@unict.it
2   CoNISMa—Consorzio Interuniversitario per le Scienze del Mare, Piazzale Flaminio, 9, 00196 Roma, Italy
3   Hellenic Centre for Marine Research (HCM), Institute of Marine Biology, Biotechnology and Aquaculture (IMBBC), 71003 Heraklion, Crete, Greece; vgerovas@hcmr.gr
4   Natural History Museum, University of Oslo, Blindern, P.O. Box 1172, 0318 Oslo, Norway
*   Correspondence: e.d.martino@nhm.uio.no

check for updates

Abstract: Investigation of bryozoan faunas collected in two submarine caves in Lesvos Island, Aegean Sea revealed a great number of colonies of three species currently assigned to the cheilostome family Onychocellidae: *Onychocella marioni* Jullien, 1882, *O. vibraculifera* Neviani, 1895, and *Smittipora disjuncta* Canu & Bassler, 1930. All species were first described and subsequently recorded on several occasions, from the Mediterranean Sea, particularly from the Aegean Sea. The availability of this material provided the basis for more detailed observations and first scanning electron microscopy (SEM) study of some diagnostic characters, including ovicells and ancestrulae, for the well-known species, as well as a few colonies of a species left in open nomenclature (i.e., Onychocellidae sp. 1) in previous works. In this paper we (*i*) update the descriptions of these four species; (*ii*) resurrect the species *Floridinella arculifera* Canu & Bassler, 1927, which was previously synonymised with *Caleschara minuta* (Maplestone, 1909), suggesting for it the new combination *Tretosina arculifera*; (*iii*) and introduce the new genus *Bryobifallax* for *S. disjuncta*.

1. Introduction

The Mediterranean Sea is one of the best studied marine areas in the world. The first, pioneering investigation started at the end of the 16th century with naturalists, such as Ferrante Imperato, also describing some bryozoan species [1]. The Mediterranean Sea hosts a high proportion of the global biodiversity with approximately 17,000 species [2], including 556 bryozoans which account for about 10% of the world known diversity for the phylum [3]. However, large sectors (mostly in the eastern and southern Mediterranean) and several habitats (e.g., remote and hardly accessible dark habitats) remain understudied, as recently demonstrated [4–8].

In this context, the availability of samples from submarine caves of Lesvos Island, located in the northeastern sector of the Aegean Sea in the NE Mediterranean, was twofold relevant because they yielded colonies of both rare and undescribed taxa (e.g., [6]).

Here, we focus on species of the family Onychocellidae or onychocellid-like taxa. The family Onychocellidae was introduced by Jullien [9] based on *Onychocella* Jullien, 1882, the type species of the genus, for species having autozooids with extensive cryptocyst, opesiae placed in the autozooidal distal half and lacking spines, inconspicuous ovicells, and large polymorphs (or onychocellaria)

whose mandibles typically show unpaired or paired cuticular wings (see also [10]). The family presently includes 33 genera [10] but only two (with four species in total) are currently recorded in the Mediterranean [3,11–13]. These are: *Onychocella* with three species, i.e., *O. marioni* Jullien, 1882, *O. angulosa* (Reuss, 1848), and *O. vibraculifera* Neviani, 1895; and *Smittipora* Jullien, 1882, i.e., *S. disjuncta* Canu & Bassler, 1930, a problematic species sometimes attributed to *Rectonychocella* Canu & Bassler, 1917, another onychocellid genus, long considered as a synonym of *Smittipora*.

Only *O. marioni* has been extensively reported from the whole basin (with putative records from the Atlantic), whereas the remaining species have rarely been recorded, the latter two species usually only with a few colonies essentially from the Aegean Sea [4,5,14–18]. However, modern descriptions and SEM imaging are scarce or missing for all mentioned species.

Onychocellids have large and thick zooids and are easily detectable when sorting samples, even with the naked eye. However, their simple morphology with very few and poorly species- and genus-diagnostic characters (e.g., [10]), can cause a certain confusion between species that can be genuinely considered Onychocellidae and onychocellid-like taxa.

This paper aims to describe and illustrate these four Mediterranean "onychocellid" species from new material collected in two submarine caves of Lesvos Island (Greece), and we here suggest a new combination for two of these species which are also displaced from the family Onychocellidae and introduce a new genus for one of them.

2. Material and Methods

The material studied here was mainly collected in two submarine caves formed in Triassic carbonate rocks on the southeastern coast of Lesvos Island, N Aegean Sea, Greece. These are: Fara cave (38.969° N, 26.477° E), a 32-m-long branch of a cave complex, and Agios Vasilios cave (38.969° N, 26.541° E), a 25-m-long funnel-shaped blind cave. Both caves have been widely studied for their morphology and for some taxonomic groups of the sessile benthic component [4,19–22]. A summary of the samples collected at Lesvos, with the number of colonies of the four target species yielded in each cave, can be found in Table 1.

Table 1. List of onychocellid *s.l.* species and their distribution in the Fara and Agios Vasilios caves of Lesvos Island, NE Aegean Sea.

Cave	Fara Cave			Agios Vasilios Cave			
Cave depth (m)	11–18			24–40			
Sampling station	F3	FC2	F4	VC1	V1	VC2	V2
Sample location inside caves	Walls	Ceiling	Walls	Ceiling	Walls	Ceiling	Walls
Distance from the entrance (m)	5–10	15–20	20–30	5–10	5–10	15–20	15–20
Depth (m)	17	15	17	25	30	27	30
Biocoenosis	SD	Trans	Dark	SD	SD	Dark	Dark
Dominant encrusters	Sc-Sp	Sr-B	Sr-Sp	Sc-Sp	Sp	Sc-Sp-Sr	Sp-Sr
Onychocella marioni Jullien, 1882	1 (1)	17 (4)	20 (10)	6 (3)	17 (12)	12 (4)	34 (14)
Onychocella vibraculifera Neviani, 1895		2	6 (1)				
Bryobifallax disjuncta (Canu & Bassler, 1930)					4 (1)		2 (1)
Tretosina arculifera (Canu & Bassler, 1927)			3 (2)			(1)	

For each species, the number of living and dead colonies (in brackets) is indicated. For each station the following data are reported: sampling location either on the Walls or Ceiling of the cave; distance from the entrance and approximate depth (in metres); biocoenosis and main encrusters indicated by the following abbreviations: SD = Semidark Cave Biocoenosis; Trans = Transitional Zone; Dark = Dark Cave Biocoenosis; Sc = Scleractinian corals; Sp = Sponges; Sr = Serpulid Polychaetes; B = Bryozoans.

Additional *Onychocella* colonies were collected in three submarine caves located at about 20 m depth in the Plemmirio Marine Protected Area (SE Sicily, western Ionian Sea). Detailed information for these samples can be found in Rosso et al. [23].

Samples were routinely processed at the Palaeoecological Laboratory of the Department of Biological, Geological and Environmental Sciences (DSBGA), University of Catania (Italy). They were washed and sieved, bryozoan colonies and fragments picked, and species initially identified using

a stereomicroscope. Selected, uncoated colonies were imaged with a TESCAN-VEGA-LMU SEM, using low-vacuum and backscattered electrons, at the Microscopical Laboratory of DSBGA.

Measurements were taken from SEM images using the image processing program ImageJ (available from https://imagej.nih.gov/).

The material is deposited in the Rosso Collection at the Palaeontological Museum of the University of Catania (PMC) under the catalogue numbers reported for each species.

3. Systematic Account

Superfamily Microporoidea Gray, 1848.

3.1. Family Onychocellidae Jullien, 1882

Genus *Onychocella* Jullien, 1882.
Type species.
Cellepora angulosa Reuss, 1848, by subsequent designation [24] (p. 388). Miocene, Austria.

3.1.1. *Onychocella marioni* Jullien, 1882
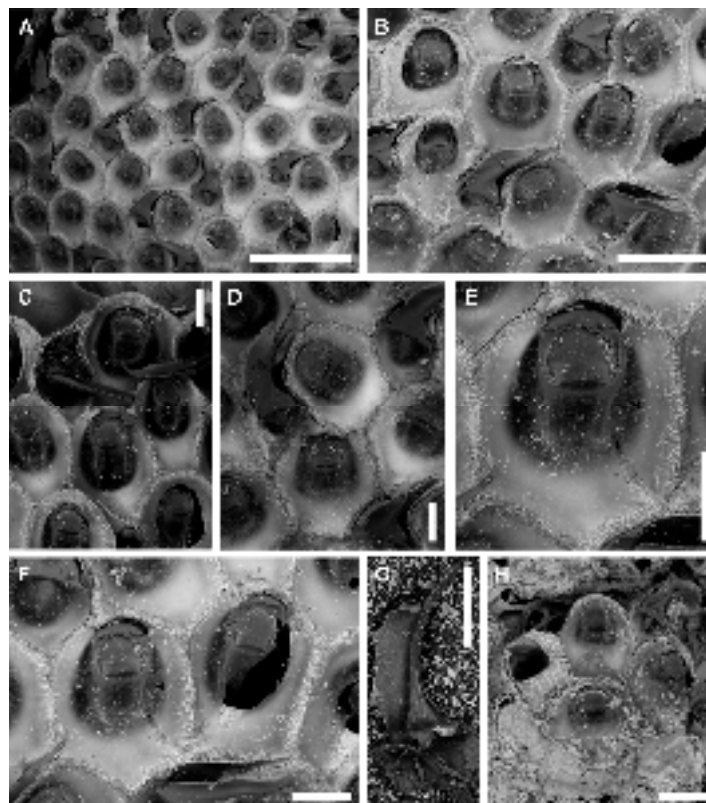
(Figures 1–3, Table 2)

Figure 1. *Onychocella marioni* Jullien, 1882. Unbleached colony (collected alive) with organic tissues and frontal membranes. Sample V1A, from the walls of the Agios Vasilios cave. (**A**–**G**): PMC. Rosso Collection GR.H. B-11e-1. (**A**) General appearance. Note the great number of vicarious avicularia. (Scale bar: 1 mm). (**B**) Some autozooids with ooecia and avicularia. (Scale bar: 500 μm). (**C**) Close-up of autozooids and avicularia from the colony margin. (Scale bar: 200 μm). (**D**) Ovicellate autozooid with cormidial ooecium produced by the distal autozooid and avicularium. (Scale bar: 200 μm). (**E**) Close-up of an ovicellate autozooid with closed operculum. (Scale bar: 200 μm). (**F**) Autozooids, one slightly inclined, with ooecia as barely visible, crescentic-like fissures. (Scale bar: 200 μm). (**G**) Basal view of a detached mandible. (Scale bar: 200 μm). (**H**) PMC. Rosso Collection GR.H. B-11e-2. Ancestrula and first budded autozooids, one distally and two distolaterally. (Scale bar: 200 μm).
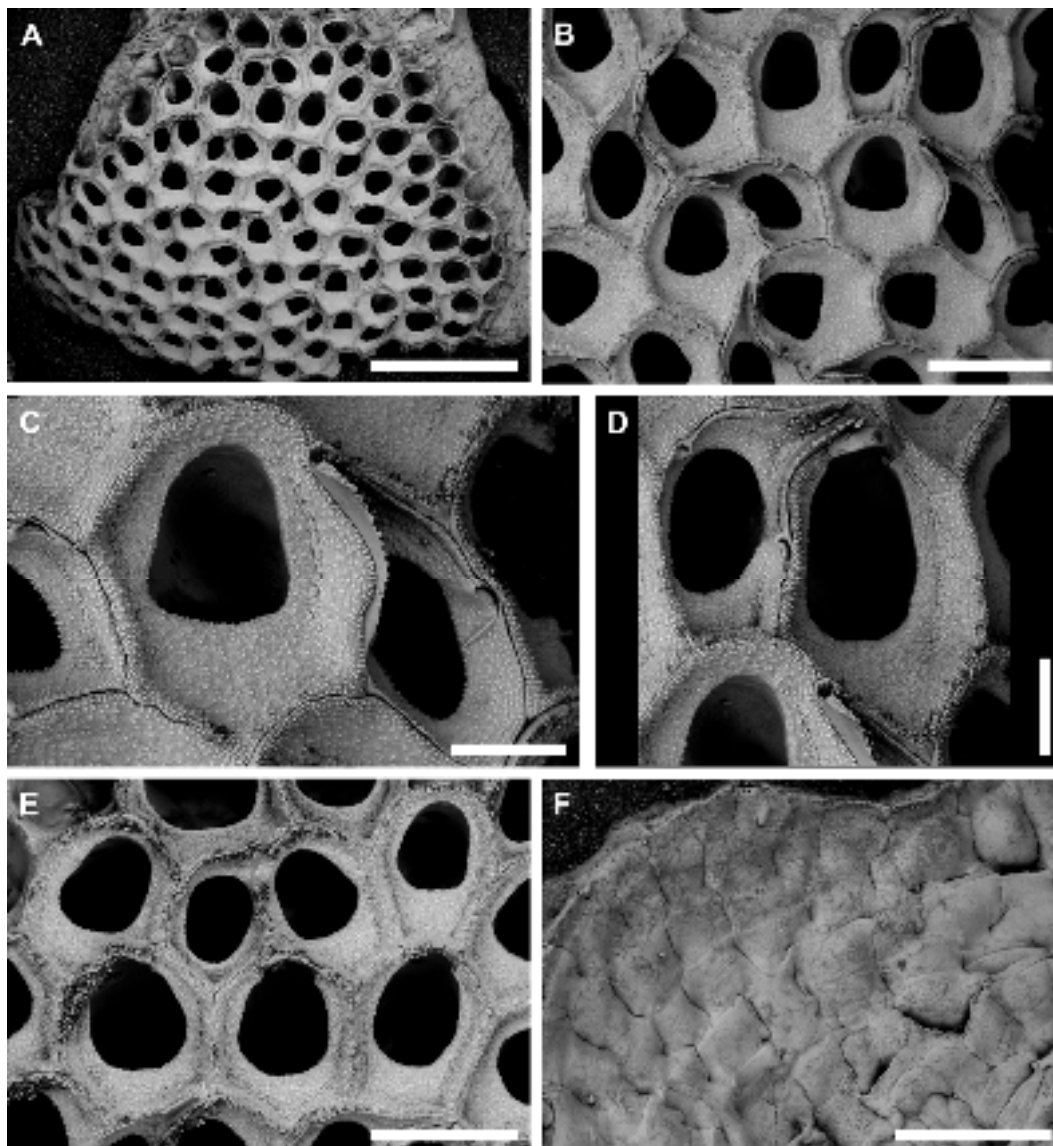
Figure 2. *Onychocella marioni* Jullien, 1882. Variability of zooidal characters. Bleached colonies from the walls of the Agios Vasilios cave. (**A–E**) PMC. Rosso Collection GR.H. B-11e-1. Sample V1A. (**A**) Colony lobe with peripheral growing margin showing the variability in the development of the cryptocyst and in the size and shape of the opesia. (Scale bar: 1.5 mm). (**B**) Close-up of the transitional zone with earlier autozooids on the right bottom corner. (Scale bar: 500 μm). (**C**) Autozooid with semielliptical opesia distally bordered by a rim of cryptocyst, and vicarious avicularium with serrated rostrum and lateral scars to hinge the mandible. (Scale bar: 200 μm). (**D**) Ovicellate autozooid with cup-shaped, gymnocystal ooecium. (Scale bar: 200 μm). (**E**) Marginal zooids, some with vestigial ooecia (bottom row) and some with incomplete cryptocyst and consequently larger opesiae (top row). (Scale bar: 500 μm). (**F**) Dorsal view of a laminar expansion with indefinite proximal and distal margins and lateral boundaries marked by thin furrows. Sample V2B. PMC. Rosso Collection GR.I.H. B-11e-3. (Scale bar: 1 mm).

Synonymies

Onychocella marioni Jullien 1882 [9] (p. 277, text-fig. unnumbered); Canu & Bassler 1930 [25] (pl. 1, figs 11, 12); Prenant & Bobin [12] (fig. 95); Rosso 1996a [26] (tabs 2, 5, pl. 1, fig. b); Di Geronimo et al. 2001 [27] (fig. 3E); Rosso et al. 2013a [23] (tab. 17.1); Rosso et al. 2013b [28] (tab. 1); Chimenz Gusso et al.

2014 [16] (p. 45, fig. 45a–c); Rosso et al. 2019a [4] (figs 2F and 3B,C, tab. 1, pars) Achilleos et al. 2020 [8] (fig. 2H, Table 1).

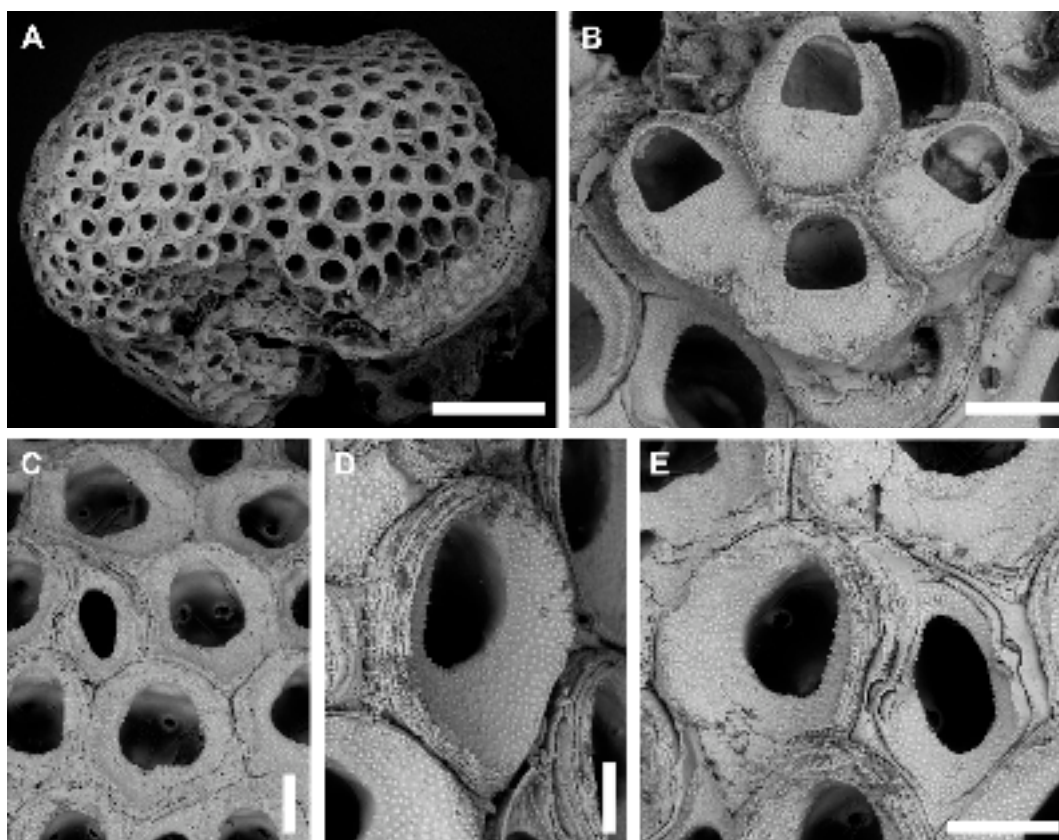O. angulosa Hayward 1974 [15] (p. 372, fig. 2A).

Figure 3. *Onychocella marioni* Jullien, 1882. Multilayered growth and regenerations. Bleached colonies from the walls of Agios Vasilios cave. PMC. Rosso Collection GR.H. B-11e-4. Sample V2C. (**A**) Multilayered colony with evidence of self-overgrowth of lobes generated from pseudoancestrulae. Note the great number of vicarious avicularia. (Scale bar: 1.5 mm). (**B**) Ancestrula and periancestrular triad of zooids fouling a colony of the same species. (Scale bar: 200 μm). (**C**) Group of zooids with uniporous septula located basally on the distal walls. (Scale bar: 200 μm). (**D**) Regenerated autozooid with multiple (at least seven) cryptocystal rims. (Scale bar: 100 μm). (**E**) Regenerated autozooids and avicularium. (Scale bar: 200 μm).

Material Examined

Aegean Sea, Lesvos Island: Fara cave (Table 1): sampling station F3, semidark cave wall, one living and one dead colony; station F4, dark cave wall, 20 living and 10 dead colonies; station FC2, ceiling at the transition between semidark and dark cave sectors, 17 living and four dead colonies; Agios Vasilios cave: station V1, semidark cave wall, 17 living and 12 dead colonies; station V2, 34 living and 14 dead colonies; station VC1, six living and three dead colonies; station VC2, ceiling in the dark cave sector, 12 living and four dead colonies. PMC, Rosso Collection, deposited under the collective code: PMC. Rosso Collection GR.H. B-11e. Additional material: Ionian Sea, Plemmirio Peninsula (Sicily), Granchi, Gymnasium and Mazzere caves: PMC. Rosso Collection I.H. B-11a.

Description

Colony encrusting, multiserial, uni- to multilaminar, moderately large, up to 5–6 cm^2 in the examined material, forming knobs of self-overgrowing lobes produced by pseudoancestrulae budded frontally by scattered autozooids (Figures 2A and 3A) of the outer layer; occasionally producing

unattached laminar extensions up to one cm in length; light brown with dark brown avicularian mandibles when alive.

Table 2. Measurements of *Onychocella marioni*, Jullien, 1882 and *Onychocella vibraculifera* Neviani, 1895.

Species	*Onychocella marioni*	*Onychocella vibraculifera*
	Jullien, 1882	**Neviani, 1895**
Zooid length	457.67–633.84; 537.72 ± 49.26 (n = 20)	372.33–477.72; 426.97 ± 27.57 (n = 20)
Zooid width	376.88–527.94; 441.68 ± 37.86 (n = 20)	233.27–388.75; 325.67 ± 34.09 (n = 20)
L/W	1.22	1.31
Opesial length	226.63–312.37; 274.69 ± 24.60 (n = 20)	127.28–216.33; 174.41 ± 25.89 (n = 20)
Opesial width	201.57–281.54; 233.44 ± 23.35 (n = 20)	134.48–191.81; 165.39 ± 18.76 (n = 20)
Ovicellate zooidal length	574.89–685.52; 620.34 ± 37.82 (n = 8)	430.80–472.63; 450.56 ± 16.65 (n = 5)
Ovicellate zooidal width	415.24–607.05; 525.30 ± 60.95 (n = 8)	314.49–352.17; 336.03 ± 13.78 (n = 5)
Ovicellate zooid opesial length	382.62–422.59; 401.92 ± 15.14 (n = 8)	150.42–231.93; 196.51 ± 37.55 (n = 5)
Ovicellate zooid opesial width	207.64–345.15; 303.19 ± 45.51 (n = 8)	167.23–205.84; 183.16 ± 15.95 (n = 5)
Ooecium length	42.04–47.69; 44.87 ± 4.00 (n = 2)	55.96–59.56; 58.31 ± 2.04 (n = 3)
Ooecium width	150.32–205.11; 177.72 ± 38.74 (n = 2)	110.52–189.21; 141.73 ± 41.79 (n = 3)
Avicularium length	435.83–729.55; 566.61 ± 69.09 (n = 20)	285.24–419.75; 363.63 ± 62.80 (n = 5)
Avicularium width	244.06–393.10; 315.07 ± 39.96 (n = 20)	184.00–239.27; 209.69 ± 21.78 (n = 5)
Avicularium opesial length	214.57–366.37; 267.31 ± 40.66 (n = 20)	147.95–173.69; 158.98 ± 11.78 (n = 5)
Avicularium opesial width	132.58–224.46; 170.64 ± 25.16 (n = 20)	63.71–94.01; 79.73 ± 12.39 (n = 5)
Ancestrula length	326.13–353.02; 359.58 ± 19.01 (n = 2)	213.23
Ancestrula width	399.70–426.12; 412.91 ± 18.68 (n = 2)	191.32
Ancestrula opesial length	157.57	128.22
Ancestrula opesial width	168.82	117.66
Tubercle diameter	Absent	33.80–69.96; 54.35 ± 11.45 (n = 10)

Abbreviations: L, length; W, width. Measurements are given in µm, as ranges and mean values ± standard deviation, followed by the number of measurements made in brackets.

Autozooids irregularly or quincuncially arranged, communicating through few, large septular pores located at mid-height on the vertical walls (Figure 3C); large (mean ± Standard Deviation: 538 ± 49 × 442 ± 38 µm) and thick, generally slightly longer than wide (mean L/W: 1.22) but often as long as wide (Figures 1B and 2E); hexagonal, often arched distally; zooidal boundaries raised, with a median groove in between (Figure 2B,C and Figure 3D,E). Gymnocyst absent. Cryptocyst (Figures 2 and 3) more extensive proximally, narrowing laterally to the opesia, tapering distally; concave and sloping towards the opesia; evenly and coarsely granular with granules smaller and more densely packed along the margins.

Opesia distal but not terminal (mean ± SD: 275 ± 25 × 233 ± 23 µm), highly variable in size and shape depending on ontogeny (Figure 2A,B and Figure 3A), longer than wide, roundish to semielliptical, with a straight to slightly concave, granular proximal border. Frontal membrane covering the whole surface in living colonies. Operculum monomorphic (Figure 1A–E), sensibly smaller (mean ± SD: 139 ± 7 × 158 ± 9 µm) than the opesia and very distally placed.

Ovicell immersed, acleithral; ooecium either small (mean ± SD: 45 ± 4 × 178 ± 39 µm), cap-shaped with proximal gymnocystal edge (Figure 2D), distal cryptocystal area and no evidence of a median suture, or more often vestigial, visible as an arched fissure above the opesia (Figure 1F), produced by the distal autozooid or cormidial, resulting from two distal autozooids or an autozooid and an avicularium (Figure 1D). Spines absent.

Avicularia common (avicularium–autozooid ratio 1:2.5 and 1:4 in the two examined colonies including about 100 zooids each), vicarious, as long as autozooids but narrower (mean ± SD: 567 ± 69 × 315 ± 40 µm), strongly arched and asymmetrical; gymnocyst usually restricted to the lateral raised walls of the rostrum and occasionally developed proximally if an ovicell is present (Figure 1B–D, Figure 2C–E and Figure 3E); cryptocyst extensive, similar in appearance to the cryptocyst of autozooids; opesia subcentral, elliptical (mean ± SD: 267 ± 41 × 171 ± 25 µm), the margin beaded as a result of the cryptocystal granules projecting into it; rostrum triangular, about half of the total length of the avicularium with elevated, serrated margins; two delicate knobs with C-shaped fissures at

mid-opesia length as a hinge for the mandible. Mandible triangular and falciform, slightly hooked, about 420 μm long, with a median arched sclerite and extensive lateral wings on the convex side. Ancestrula similar to a normal zooid but smaller (mean ± SD: 360 ± 19 × 413 ± 19 μm), budding one distal and two disto-lateral autozooids of about the same size (Figures 1H and 3B).

In a few colonies, unilaminar expansions extend up to 1 cm over the substrate showing the slightly swollen basal walls of the zooids, their arrangement in somewhat radial rows marked by thin furrows and zooidal lateral connections (Figure 2F).

Intramural budding common in both autozooids and avicularia, with multiple regenerations visible as piled-up zooidal rims, up to seven in the examined material (Figure 3C–E).

Remarks

In the colonies examined, peripheral autozooids appear larger and with wider, roundish to elliptical opesiae compared to autozooids placed in other regions of the colony. Differences in the description of these characters and the wide ranges of zooidal and opesial measurements reported in the literature (e.g., [9,11,12,16]) can be explained by the high ontogenetic variability, as already noted by previous authors. The few morphological features available to distinguish species of *Onychocella* (see also discussion in [29] p. 40), and the high intraspecific and intracolonial variability, possibly contributed to a proliferation of species and confusing synonymies often merging together fossil and living taxa.

In addition to *Onychocella vibraculifera* Neviani, 1895 (described below), at least three more species have been reported from the Atlanto-Mediterranean area: *O. marioni* described from recent material from the NW Mediterranean; *O. antiqua* (Busk, 1858) described from living specimens from Madeira; and *O. angulosa* Reuss, 1848, described from European Cenozoic material. Taylor et al. [10] summarised the problems related to the synonymy of the fossil species with the modern taxa and the urge for a revision of the type material to assess possible conspecificity. In the Mediterranean, *O. antiqua* was reported only once from Turkish waters [30] and its genuine occurrence was questioned in Rosso & Di Martino [3]. Based on Reuss' drawings [31] (pl. 11, fig. 10), *O. angulosa* would differ from *O. marioni* in having autozooids with centrally placed, polygonal opesiae, and small heterozooids with reduced opesiae. These potential differences, that can be also observed in specimens of *O. angulosa* illustrated in Zágoršek [32] (pl. 62), prevent the assessment of the long presumed conspecificity between *O. angulosa* and *O. marioni* without a careful examination of the type material. Further records from present-day west Africa by Cook [33] (p. 68, fig. 11A,B) seemingly point to a different species showing a distal orificial process projecting into the opesia. Here, we prefer to refer our specimens to *O. marioni* because of the above-mentioned morphological differences and because the material studied is recent. *Onychocella marioni* differs from the Mediterranean congener *O. vibraculifera* in the colour of the living colonies and in the additional skeletal characters discussed below.

We provide the first SEM images of the ancestrula with the first three budded zooids (one distally and two distolaterally), a configuration more commonly observed than the ancestrula alone or with a single distal zooid. Ancestrulae without buds were never described or illustrated for this species, suggesting a possible immediate budding of the first zooid. This is in agreement with observations made by Cook [34] on *Onychocella alula* Hastings, 1930, in which fully calcified walls of the primary bud were observed after 12 h, while distolateral buds appeared after 108 h from larval settlement. The ancestrula was first described by Canu & Bassler [25] as a "small ordinary zooid". After Gautier [35] erroneously figured an isolated tatiform ancestrula encrusting the lateral proximal wall of the real ancestrula of *O. marioni*, Gautier [11] himself and other authors, such as Prenant & Bobin [12], described the ancestrula as being either tatiform or similar to a later autozooid, while Zabala [36] reported only a tatiform ancestrula with 11 spines.

Colonies of *O. marioni* from Lesvos caves form nodular, multilayered, elevated structures [4] similar to those described by Harmelin [37] from the Trémies cave (Marseille area, France). This species also formed small pillar-shaped structures in a shallow-water, dark cave from Lebanon [J.-G. Harmelin,

personal communication, October 2020]. Harmelin [37] discussed the perenniality of this species, which is able to maintain the colonised space through the superimposition of subsequent layers, creating new cryptic space for smaller, less competitive species growing around the nodules. In some colonies, we also observed frontal budding with the formation of pseudoancestrulae produced mainly by autozooids.

Unilaminar expansions were never reported in *O. marioni* to date, and never observed in colonies from submerged caves, although sometimes found in colonies from deep shelf biodetritic bottoms in the Ionian Sea, off eastern Sicily (AR, personal observations). In marine cave habitats, the development of these marginal laminae may allow the colony to overtop neighbouring organisms, an unusual strategy for a species with intrazooidal budding but seemingly advantageous on locally highly colonised hard surfaces such as the walls and ceiling of the caves.

Distribution

Based on the comments above (see Remarks) and adopting the same approach as in Berning [29] (p. 42) for *O. angulosa*, we refrain from providing a detailed, general distribution of *O. marioni*. Although recorded from the Atlantic around the Iberian Peninsula [38], it is likely that *O. marioni* is an endemic Mediterranean species, widely distributed on the whole basin. It has been commonly found in several localities and habitats by one of us (AR) including: coralligenous concretions at 35–55 m depth in the Gulf of Noto, SE Ionian coast of Sicily [39] and pillar-like coralligenous structures at 30 m depth in the same area [26,40]; circalittoral detritic bottoms in the Gulf of Noto (33–78 m living and 33–83 dead) [26], detritic bottoms of the outer shelf in the Ciclopi Island Marine Protected Area (AR, personal observations), and off Ustica Island (60 m living and dead) [41,42]; several submarine caves from the Ionian coast of Sicily [23,28,43]. Additional plausible records are from: Marseille area [9] and other localities along the Mediterranean French coast in: coralligenous habitats, dark and semidark caves, and clastic biogenic bottoms [11,35,44,45]; including the underside of small substrata [45,46] underwater tunnels in Medes Island, Catalan coast [47]; off the coast of Latium, Volcano Isle (S Tyrrhenian Sea), Tunisia [16]; the Aegean Sea in the Karpathos Strait (29–80 m), Kythira Island (66 m) and Santorini (100–128 m) [14]; localities along the southern coast of Chios Island, i.e., Cape Masticho (15–60 m), Venetiko (12–50 m), and Emborios Bay (1–15 m) but reported as *O. angulosa* [15], and off Milos Island [48]; Cyprus [8,49], and the coasts of Turkey [50] and Lebanon [18].

3.1.2. *Onychocella vibraculifera* Neviani, 1895
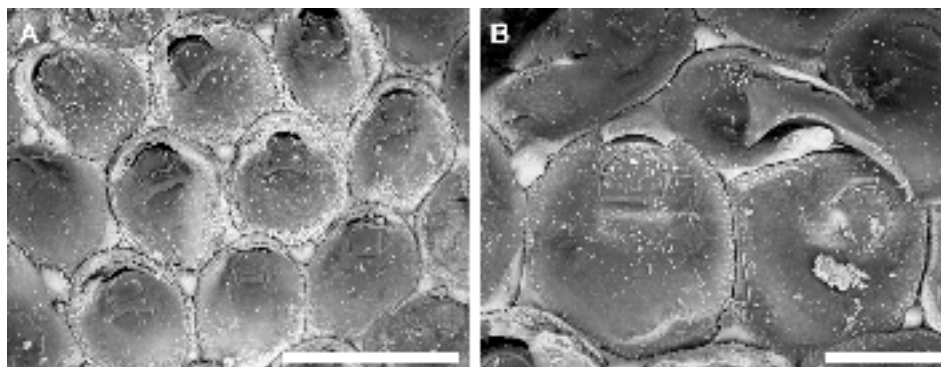
(Figures 4–6, Table 2)

Figure 4. *Onychocella vibraculifera* Neviani, 1895. Unbleached colony (collected alive) with organic tissues and frontal membranes. PMC. Rosso Collection GR.H. B-16b-1. Fara cave. Sample F4C. (**A**) Group of autozooids with well-developed gymnocystal tubercles located at zooidal triple junctions. (Scale bar: 500 μm). (**B**) Close-up of two zooids, one ovicellate, showing the transversely D-shaped outline of the operculum, and a vicarious avicularium with curved and hooked mandible. (Scale bar: 200 μm).
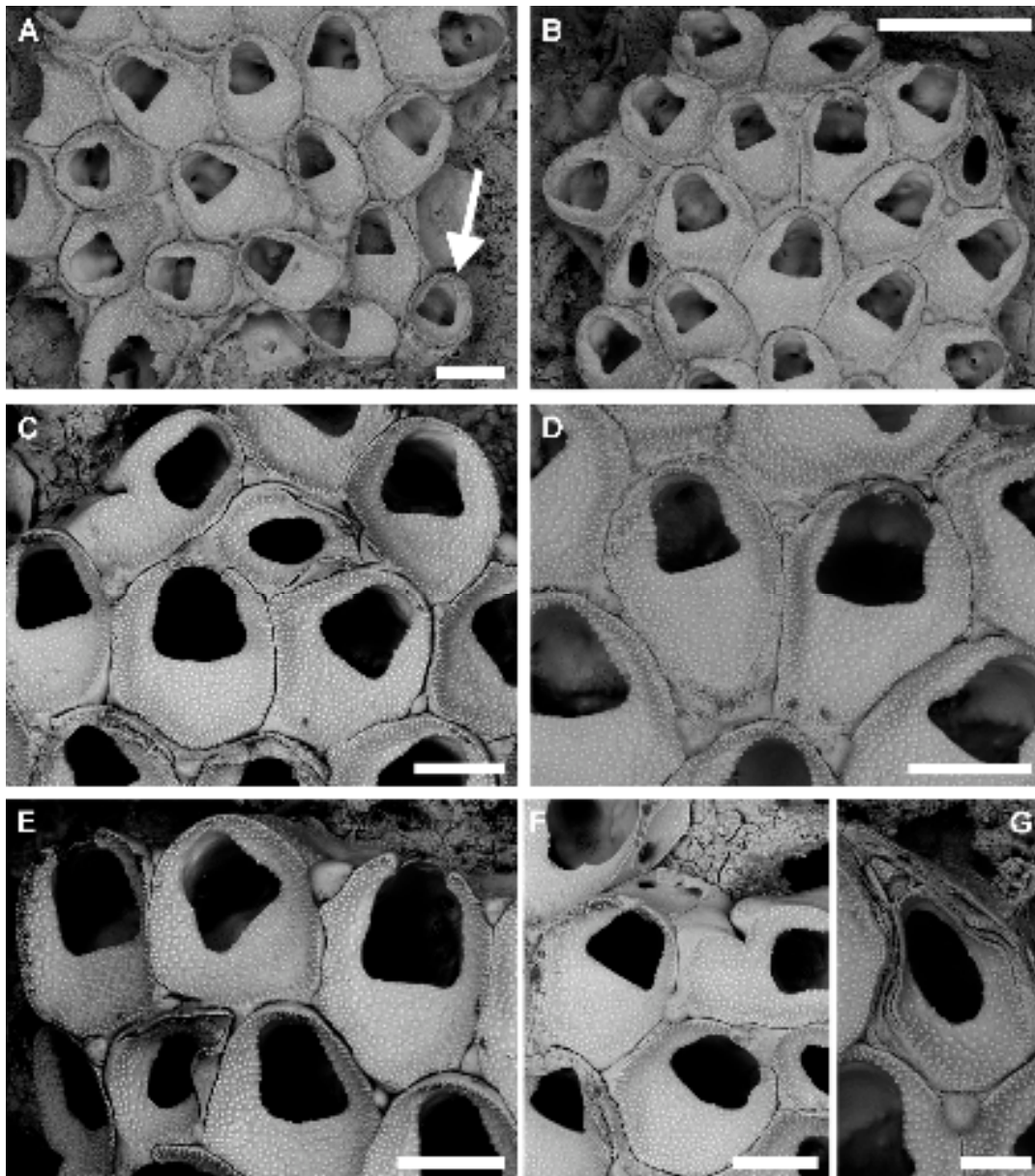
Figure 5. *Onychocella vibraculifera* Neviani, 1895. Bleached colonies from the walls of the Fara cave. PMC. Rosso Collection GR.H. B-16b-1. Sample F4C with C and F also shown in Figure 4. (**A**) Group of zooids from a young colony. The putative ancestrula (or first budded autozooid) is visible on the bottom right corner (arrowed). (Scale bar: 200 μm). (**B**) Distal lobe of the same colony showing autozooids and vicarious avicularia with multiple cryptocystal rims due to intramural budding. (Scale bar: 500 μm). (**C**) Close-up of two zooids, one ovicellate, and a vicarious avicularium contributing to the formation of the gymnocystal ooecium (same as in Figure 4B). Note the slightly dimorphic opesia of the ovicellate zooid. A teratologic zooid is visible on the left top corner. (Scale bar: 200 μm). (**D**) Close-up of two zooids in B. The ovicellate zooid (on the right side) shows the vestigial ooecium with associated dimorphic opesia, which is terminally placed and larger compared to that of the non-ovicellate zooid. (Scale bar: 200 μm). (**E**) Peripheral autozooid, two with forming ooecia appearing as thin arches interrupting the distal cryptocystal rim. (Scale bar: 200 μm). (**F**) Inclined view of the left side of C, showing uniporous septula along lateral and distal walls. (Scale bar: 200 μm). (**G**) Close-up of an avicularium with evidence of multiple intramural budding. (Scale bar: 100 μm).
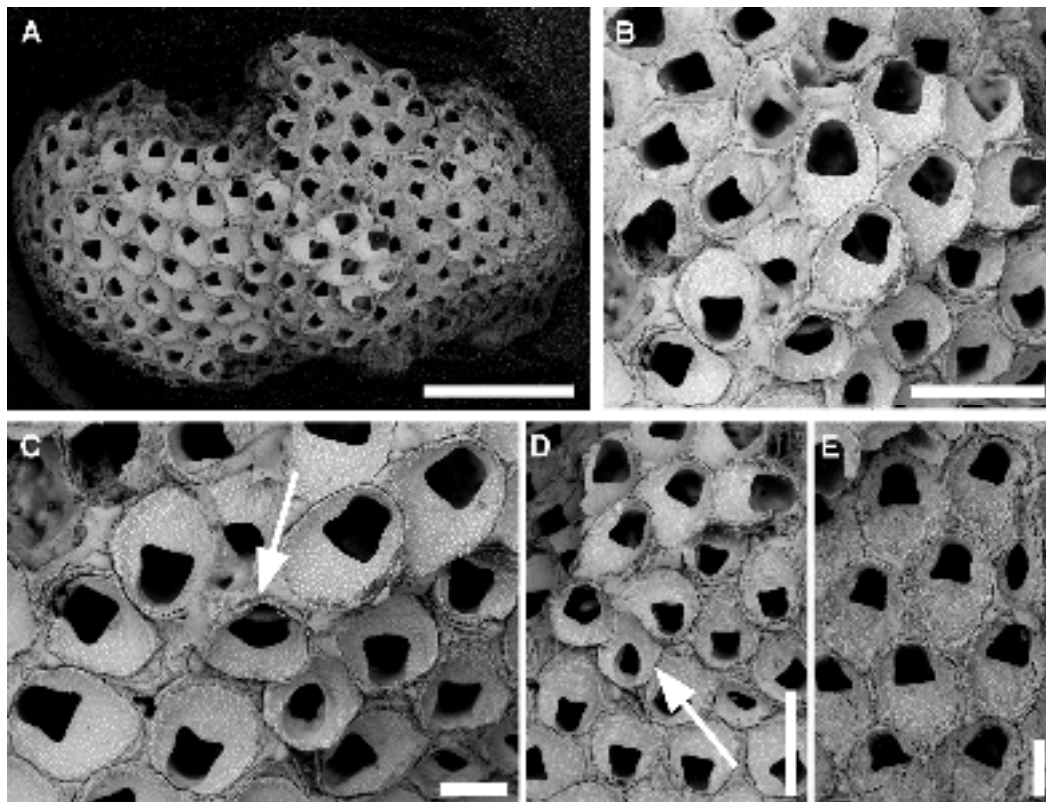
Figure 6. *Onychocella vibraculifera* Neviani, 1895. Multilayered growth, regenerations, and reproduction. Bleached multilayered colony from the wall of Fara cave. PMC. Rosso Collection GR.H. B-16b-2. Sample F4A. (**A**) Multilayered colony forming a slightly elevated knob. Note that vicarious avicularia are rare. (Scale bar: 1.5 mm). (**B**) Group of autozooids from the outermost layer, some ovicellate. (Scale bar: 500 μm). (**C**) Chaotically arranged autozooids, with frequent regeneration via intrazooidal budding, from a new layer starting from a pseudoancestrula (arrowed). (Scale bar: 200 μm). (**D**) Frontal view of the pseudoancestrula in (**C**), originating from a regenerated avicularium (arrowed) and budding two proximolateral autozooids with opposite growth directions. (Scale bar: 500 μm). (**E**) Zooids, one ovicellate, from the underlying, partly exposed layer; the ooecium is formed by the distal avicularium. (Scale bar: 200 μm).

Synonymies

Onychocella vibraculifera Neviani 1895 [51] (p. 97, pl. 5, fig. 6); Gautier 1962 [11] (p. 58); Prenant & Bobin 1966 [12] (p. 293, fig. 97, 1–5); Hayward 1974 [15] (p. 374, fig. 2c); Zabala & Maluquer 1988 [13] (p. 87, fig. 109); Rosso et al. 2010 [52] (p. 599); Rosso et al. 2013a [23] (tab. 17.1); Rosso et al. 2013b [28] (tab. 1, fig. 3f); Chimenz Gusso et al. 2014 [16] (p. 111, fig. 46a–c).

Onychocella marioni Rosso et al. 2019a [4] (tab. 1, pars).

Material Examined

Aegean Sea, Lesvos Island: Fara cave: sampling station F4 (Table 1), dark cave wall, one dead and six living colonies; station FC2, ceiling at the transition between semidark and dark cave sectors, two living colonies. Deposited under the collective code: PMC. Rosso Collection GR.H. B-16b. Additional material: Ionian Sea, Plemmirio Peninsula (Sicily), Gymnasium and Mazzere caves: few dead colonies: PMC. Rosso Collection I.H. B-16a.

Description

Colony encrusting, multiserial, uni- to paucilaminar, usually small sized (<1 cm^2) in the examined material, forming small patches or knobs (Figures 5A and 6A) of self-overgrowing lobes produced by

pseudoancestrulae budded frontally by scattered autozooids or, more often, avicularia (Figure 6B–D) of the outer layer; whitish-beige when alive, with darker spots corresponding to sclerites of the avicularian mandibles.

Autozooids irregularly or quincuncially arranged, large (mean ± SD: 427 ± 28 × 326 ± 34 μm) and thick, slightly longer than wide (mean L/W: 1.31); generally ovoidal but often rounded polygonal and arched distally; zooidal boundaries raised and outlined by narrow grooves (Figures 4A and 5A,B–D, Figure 6A,B,E). Gymnocyst forming the lateral walls, visible frontally only on zooidal proximal corners, mostly in irregularly growing areas (Figure 5E,F and Figure 6D). Cryptocyst (Figures 5 and 6) extensive, occupying the proximal half of the frontal surface, and forming two wings projecting laterally into the opesia at about mid-length, in a few instances tapering gradually; absent distally; depressed, gently sloping from the zooidal rim, flat centrally; coarsely and evenly granular, except for the sloping margins where granules are smaller and more densely packed.

Opesia terminal, longer than wide (mean ± SD: 174 ± 26 × 165 ± 19 μm), subtrapezoidal, with blunt corners, and a straight proximal border except in a few zooids in which is either concave or convex; dimorphic and becoming subquadrangular in ovicellate autozooids (Figure 5D,F). Frontal membrane covering the whole surface in living colonies. Muscle scars roundish, hardly visible through the opesia. Operculum monomorphic (Figure 4B), small (mean ± SD: 88 ± 3 × 102 ± 3 μm), corresponding to the distal median part of the opesia. Spines absent.

Ovicell immersed (Figure 5E); ooecium small (mean ± SD: 58 ± 2 × 142 ± 42 μm), cap-like, smooth, produced by the gymnocyst of the distal avicularium or the distal autozooid (Figure 4B, Figure 5C,F and Figure 6B). Avicularia rare (avicularium–autozooid ratio 1:17 to 1:21 in three examined colonies having 50–60 zooids each), vicarious, nearly as long as autozooids but narrower (mean ± SD: 364 ± 63 × 210 ± 22 μm), asymmetrical (Figure 4B, Figure 5C,E,G and Figure 6E); gymnocyst developing proximally only if an ovicell is present (Figures 4B and 5C) but constantly present laterally to the rostrum as two raised wings holding the mandibles in living specimens (Figures 4B and 5C,E); cryptocyst extensive, similar in appearance to the cryptocyst of autozooids; opesia subcentral, elliptical (mean ± SD: 159 ± 12 × 80 ± 12 μm); rostrum triangular, about half the length of the avicularium; a symmetrical arched fissure placed at opesia mid-length, at the base of the gymnocystal lateral wings as a hinge for the mandible (Figure 5C,E,G). Mandible triangular and falciform, about 300 μm long, with a median sclerite, hooked distally, largely projecting outside the rostrum (Figure 4B).

Kenozooids, as rounded tubercles (mean diameter ± SD: 54 ± 11 μm), sporadically occurring at the triple contact between zooids (Figure 4A,B and Figure 5E–G); often absent in large sectors of the colony.

Ancestrula, similar to later autozooids but smaller; presence uncertain in this material (see putative ancestrula in Figure 5A).

Regeneration via intramural budding observed mostly for avicularia (Figures 5G and 6C,E).

Remarks

Based on the morphological characters, colonies from the submarine caves of Lesvos fit well in the definition of *Onychocella vibraculifera*, but the size of the polymorphs is remarkably smaller compared to polymorph size reported in Prenant & Bobin [12] and Chimenz Gusso et al. [16] (e.g., autozooids: 520–640 × 420–480 μm).

Onychocella vibraculifera differs from *O. marioni* in having flatter cryptocyst, a smaller and more bell-shaped, terminal opesia with straight or slightly convex proximal border. Some authors sinonymised *O. vibraculifera* with *O. angulosa* Reuss, 1847 (see [12]) but the latter species lacks the interzooidal tubercles and differs also for some other morphological and morphometric characters.

Tubercles at triple zooidal junctions were also described in species of *Smittipora*, such as *Smittipora sawayai* Marcus, 1937, redescribed by Winston and Vieira [53], and *Smittipora tuberculata* (Canu & Bassler, 1928). They are apparently gymnocystal (see [10]), as in the present instance.

Distribution

Onychocella vibraculifera is an endemic Mediterranean species. It has been recorded from Tunisia [25] and the Sicily Strait [11], Aeolian Islands in SE Tyrrhenian Sea [16], SW Turkey associated with *Posidonia* rhizomes [16,50], Chios Island in Greece [15], and the coasts of Lebanon [18]. Dead colonies were also reported from submarine caves along the Ionian coast of Sicily [23,28], while both living and dead colonies were reported from the semisubmerged Accademia cave at Ustica Island, S Tyrrhenian Sea [43,54,55]. The specimens described here fall within the known geographical distribution of *O. vibraculifera*, which is restricted to the eastern and southern sectors of the Mediterranean Sea. This species occurred in the Mediterranean basin (central Italy) at least since the Pleistocene [51]. Its Pliocene record needs to be confirmed following the age updating of the deposits.

3.2. Family Microporidae Gray, 1848

3.2.1. Genus *Bryobifallax* gen. nov.
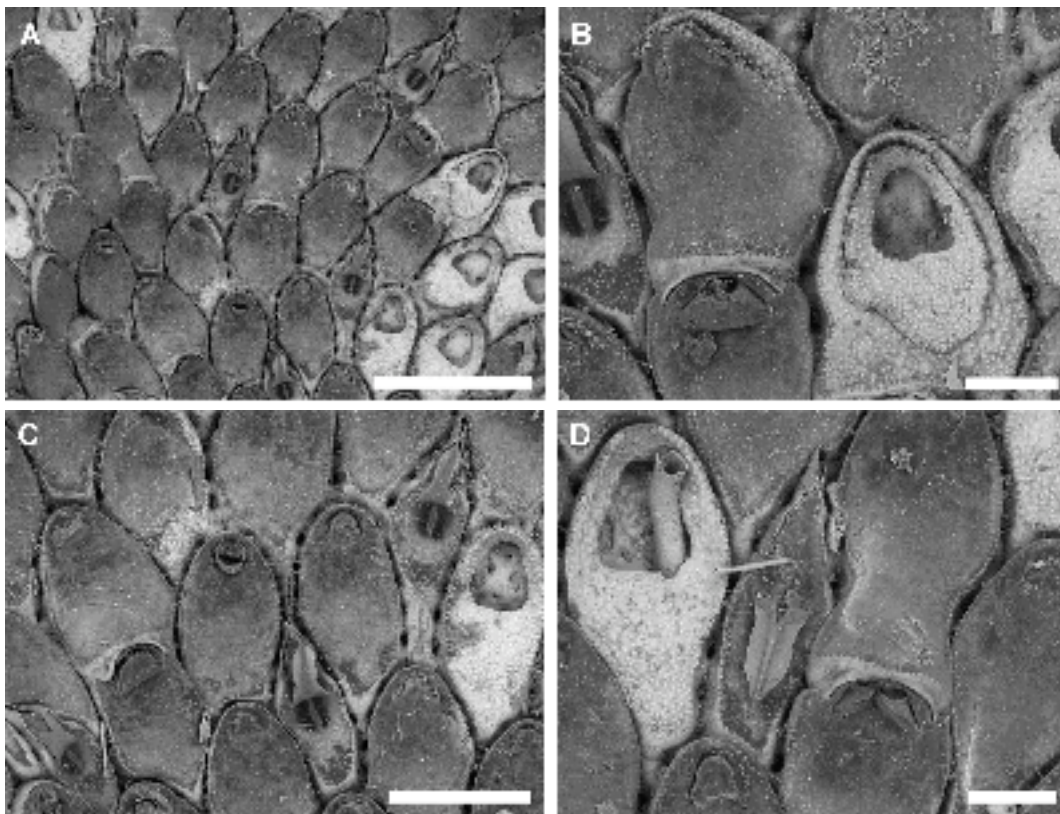
(Figures 7 and 8)

Figure 7. *Bryobifallax disjuncta* (Canu & Bassler, 1930). Unbleached colony (collected alive) with organic tissues and frontal membranes from the walls of Agios Vasilios cave. PMC Rosso-Collection GR. H. B.82a-1. Sample V1A. (**A**) General aspect. Note that some zones of the colony are occupied by dead autozooids and the regular frequency of a moderate number of vicarious avicularia. (Scale bar: 1 mm). (**B**) Close-up of an ovicellate zooid and a regenerated dead zooid. (Scale bar: 200 μm). (**C**) Group of autozooids, one ovicellate with dimorphic operculum, and avicularia with closed, flame-shaped mandibles. (Scale bar: 500 μm). (**D**) Close-up of an ovicellate zooid with associated distal autozooid producing the ooecium, and a lateral vicarious avicularium with open mandible. Note the early colonization of dead individuals by a tube-dwelling serpulid. (Scale bar: 200 μm).
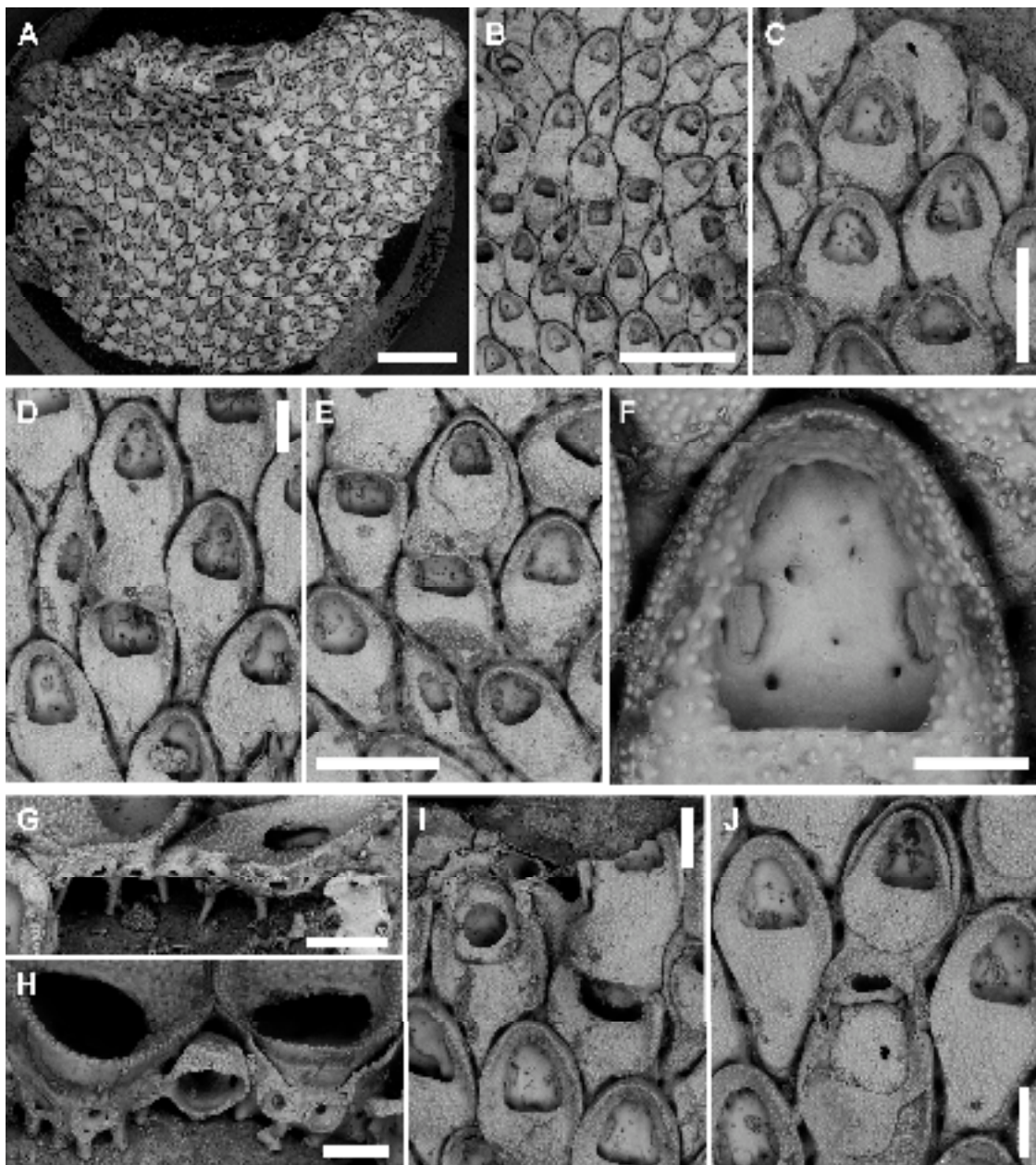
Figure 8. *Bryobifallax disjuncta* (Canu & Bassler, 1930). Bleached colony from the walls of Agios Vasilios cave. PMC Rosso-Collection GR. H. B.82a-2. Sample V1A. (**A**) General aspect. (Scale bar: 1.5 mm). (**B**) Group of zooids, some ovicellate, and vicarious avicularia. Note that the distal zooid producing the ooecium is commonly not in a coaxial position with the maternal zooid. (Scale bar: 1 mm). (**C**) Colony edge showing a large, irregularly shaped kenozooid with a small, drop-shaped opesia. (Scale bar: 500 μm). (**D**) Close-up of an ovicell complex and a vicarious avicularium. Note the dimorphic opesia. (Scale bar: 200 μm). (**E**) Ovicell complexes. One of the ooecia is produced by a regenerated distal autozooid. (Scale bar: 500 μm). (**F**) Close-up of the large semielliptical opesia showing symmetrical, longitudinally elongated muscle scars and pits corresponding to the basal pillars. (Scale bar: 100 μm). (**G**) Basal pillars. (Scale bar: 200 μm). (**H**) Inclined view of the colony growth margin showing basal pillars and zooidal communication through tubular processes. (Scale bar: 100 μm). (**I**) Colony margin showing an autozooidal opesia regenerated as a kenozooid. (Scale bar: 200 μm). (**J**) Damaged portion of the colony showing autozooids regenerated through intramural budding. The central zooid and its ooecium regenerated as kenozooids. (Scale bar: 200 μm).

Type species *Rectonychocella disjuncta* Canu & Bassler, 1930, here designated.

Diagnosis

Colony encrusting, multiserial, unilaminar, anchored to the substratum through tubular extensions. Autozooids disjointed, connected by short tubes; longer than wide, ovoidal to diamond-shaped, with a raised margin. Gymnocyst extremely reduced. Cryptocyst granular, extensive proximally and surrounding the opesia, depressed. Opesia longer than wide, semielliptical to subtrapezoidal, with a straight or gently arched proximal border; dimorphic and terminal in ovicellate zooids. Muscle scars symmetrical, visible through the opesia on the autozooidal floor. Operculum small, dimorphic. Spines absent. Ovicell subimmersed, hemisphaeric, slightly convex and gently sloping distally; the frontal surface formed by a swelling of the distal autozooid, mainly cryptocystal but with a proximal, narrow band of gymnocystal calcification arched above the opesia. Avicularia rare, vicarious, large, flame-shaped, and symmetrical, with extensive cryptocyst, pear-shaped opesia and elongate triangular rostrum with raised, gymnocystal laminae. Mandible with a straight central sclerite mirroring the shape of the rostrum. Kenozooids rare, irregularly shaped, with an extensive cryptocyst and a median small opesia.

Remarks

The new genus *Bryobifallax* is here introduced for *Smittipora disjuncta* (Canu & Bassler, 1930). This species was first placed in *Rectonychocella* Canu & Bassler, 1917, because of its symmetrical vicarious avicularia, and subsequently still mentioned as *Rectonychocella* [12,15] or included in *Smittipora* Jullien, 1882 [3,14,17,56,57]. These two genera, which share the presence of symmetrical vicarious avicularia, were considered synonyms for long time (e.g., [13]). Taylor et al. [10] clarified the differences between the two genera: *Rectonychocella* has large, ovoidal opesiae, while *Smittipora* has smaller, semielliptical opesiae with opesiular indentations. However, the type species (and other congeners) of both *Smittipora* and *Rectonychocella*, and onychocellids in general (see [10,13]), have immersed ovicells, barely visible, associated with dimorphic autozooids showing larger, cormidial opesia, in contrast with the subimmersed, escharelliform *sensu* Ostrovsky [58], ovicells of *S. disjuncta*. The occurrence of a more prominent ovicell compared to typical onychocellids, reported as "hyperstomial", was first noted by Harmelin [14] and later Hayward [15] when fertile colonies from the Aegean Sea became available. The first description of the species was in fact based on a young colony from the Tunisian coast, only consisting of periancestrular zooids. Harmelin [14] and Hayward [15] suggested displacing this species in a more suitable genus. The ovicells observed in the material from Lesvos (Figure 7B–D and Figure 8B,D,E) are reminiscent of those developed in some species of Microporidae, such as *Mollia patellaria* (Moll, 1803) from the Mediterranean Sea [16] (fig. 43d), *Micropora notialis* Hayward & Ryland, 1993 from Antarctica [59] (fig. 120D), *Flustrapora magellanica* Moyano, 1970 from Tierra del Fuego and southern Patagonia [59] (fig. 121B), [60], and especially *Coronellina atlantica* Souto, Reverter-Gil & Ostrovsky (2014) from Madeira, the latter species also sharing disjointed zooids with tubular connections [61] (figs. 4 and 5). However, because no established genera in the heterogeneous family Microporidae nor in Onychocellidae appear suitable for *S. disjuncta*, the introduction of a new genus, *Bryobifallax* gen. nov., was considered necessary. The family placement is also challenging because *Bryobifallax* gen. nov. shares features with both Onychocellidae and Microporidae. In the latter family, zooids communicate through basal pore chambers or multiporous septula, have extensive pseudoporous cryptocyst pierced by distolateral opesiules, sometimes producing opesiular indentations in the proximal border of the semicircular opesia (e.g., [59]). Furthermore, avicularia, when present, are small and usually interzooidal. However, Microporidae is here preferred to Onychocellidae because of the affinities in ovicell development.

Etymology

The name is composed by the prefixes *Bryo-* for Bryozoa and *bi-* = two times, plus the Latin adjective *fallax* = fallacious, misleading, alluding to the past erroneous inclusion of the type species in

both *Rectonychocella* Canu & Bassler, 1917 and *Smittipora* Jullien, 1982. Strictly unchanged but here assigned feminine.

3.2.2. *Bryobifallax disjuncta* (Canu & Bassler, 1930) comb. nov.

(Figures 7 and 8, Table 3).

Table 3. Measurements of *Bryobifallax disjuncta* (Canu & Bassler, 1930) comb. nov. and *Tretosina arculifera* (Canu & Bassler, 1927) comb. nov.

Species	*Bryobifallax disjuncta*	*Tretosina arculifera*
	(Canu & Bassler, 1930) comb. nov.	**(Canu & Bassler, 1927) comb. nov.**
Zooid length	481.32–701.91; 594.33 ± 64.00 (n = 20)	510.23–776.94; 648.36 ± 70.24 (n = 20)
Zooid width	278.80–406.40; 362.81 ± 28.65 (n = 20)	233.67–485.80; 418.57 ± 44.90 (n = 20)
L/W	1.64	1.55
Opesial length	184.53–257.25; 223.45 ± 21.83 (n = 20)	218.04–333.56; 282.21 ± 30.55 (n = 20)
Opesial width	180.28–233.48; 208.81 ± 14.72 (n = 20)	212.20–304.17; 263.00 ± 30.16 (n = 20)
Ooecium length	161.36–281.15; 223.06 ± 37.24 (n = 12)	210.07–319.72; 266.71 ± 54.91 (n = 3)
Ooecium width	307.71–353.94; 325.02 ± 16.81 (n = 12)	407.75–444.96; 426.17 ± 18.61 (n = 3)
Avicularium length	501.44–657.21; 574.23 ± 47.97 (n = 10)	Absent
Avicularium width	211.52–256.26; 235.47 ± 14.44 (n = 10)	Absent
Avicularium opesial length	120.92–197.04; 162.33 ± 22.47 (n = 10)	Absent
Avicularium opesial width	89.26–113.40; 102.53 ± 7.87 (n = 10)	Absent

Abbreviations: L, length; W, width. Measurements are given in μm, as ranges and mean values ± standard deviation, followed by the number of measurements made in brackets.

Synonymies

Rectonychocella disjuncta Canu & Bassler 1930 [25] (p. 21, pl. 1, fig. 8); Hayward 1974 [15] (p. 374, fig. 2b).

Smittipora disjuncta Harmelin 1969 [14] (p. 1191, fig. 2.1–2.4); Rosso et al. 2019 [5] (fig. 5d, tab. 1).

Material Examined

Aegean Sea, Lesvos Island, Agios Vasilios cave (Table 1), sampling station V1, semidark cave wall, one dead and four living colonies; station V2, dark cave wall, two living and one dead colonies. Deposited under the collective code PMC Rosso-Collection GR. H. B.82a.

Description

Colony encrusting, multiserial, unilaminar (Figure 8A), up to ca. 6 cm^2 in the observed material; in large colonies, lobes joining but rarely overlapping; anchored to the substratum through tubular extensions about 60–100 μm long and 20 μm in diameter (Figure 8G,H), visible through the opesia as pits in the autozooidal floor (Figure 8F); whitish with yellowish to hazel spots, corresponding to the avicularian mandibles, when dried.

Autozooids quincuncially arranged, large (mean ± SD: 594 ± 64 × 362 ± 29 μm), disjoint, each connected to its neighbours by numerous (ca. 16–20), short tubes barely visible in frontal view (Figures 7C and 8J); longer than wide (mean L/W: 1.64), ovoidal to diamond-shaped, arched distally, truncated bifid or tapering proximally, sometimes wedged between proximal autozooids (Figure 7A,C and Figure 8B,D,E). Marginal rim raised, especially distally and evenly beaded. Gymnocyst forming the lateral walls, usually not visible frontally except for zooidal proximal corners (Figure 7C,D). Cryptocyst coarsely and evenly granular, extensive, occupying the proximal half of the frontal surface, and completely surrounding the opesia with a band of constant width only slightly narrowing distally; depressed, gently sloping proximally to the opesia while steepening laterally and distally (Figure 8B–E,I–J).

Opesia longer than wide (mean ± SD: 223 ± 22 × 208 ± 15 μm), semielliptical to subtrapezoidal, with blunt corners and a straight or gently concave proximal border (Figure 8B–F,J); dimorphic and

becoming subquadrangular in ovicellate autozooids (Figure 8B,D,E). Frontal membrane covering the whole surface in living colonies. Muscle scars symmetrical, reniform to irregularly shaped, placed on the proximal half of the autozooidal floor visible through the opesia. Operculum small, corresponding to less than half the length and the width of the opesia; shorter but wider in ovicellate autozooids (Figure 7). Spines absent.

Ovicell subimmersed, hemispheric, formed by the enlargement and swelling of the proximal part of the distal autozooid (Figures 7 and 8B–E,I); surface slightly convex and gently sloping distally up to about half length of the frontal cryptocyst of the distal zooid, visible as a zone of more densely spaced granules compared to other frontal regions, including a distal cryptocystal endooecium and a proximal gymnocystal ectooecium consisting of a thin, protruding rim arched above the opesia marked by a band of calcification, narrow in the middle and widening laterally, with no evidence of a median suture.

Avicularia relatively rare (avicularium/autozooid ratio: 1:6.3 and 1:6.5 in colonies of 38 and 201 zooids, respectively) vicarious, about as long as autozooids but narrower (mean ± SD: 574 ± 48 × 235 ± 14 μm); symmetrical, with extensive cryptocyst, similar in appearance to the zooidal cryptocyst (Figure 7A,C,D and Figure 8B–E); opesia pear-shaped (mean ± SD: 162 ± 22 × 102 ± 8 μm); rostrum elongate triangular with the cryptocyst not fusing with the lateral, raised gymnocyst forming a flame-like margin, ending in a parallel-sided, narrow (ca. 20 × 100 μm) tip. Mandible and its straight central sclerite mirroring the flame-like shape of the rostrum gymnocyst with two lateral symmetrical membranous wings (Figure 7A,C,D).

Kenozooids rare, observed at the colony periphery, along the contact between merging lobes and in colony portions encrusting particularly irregular surfaces; slightly smaller or larger than autozooids and irregularly shaped, with extensive, granular cryptocyst with granules somewhat arranged in radial rows, and a median, subcircular to drop-shaped opesia (Figure 8C). Ancestrula not observed.

Regeneration of autozooid via intramural budding (Figure 7A,B and Figure 8E,J); kenozooids with median roundish pores budded within autozooids and ovicells (Figure 8I,J) relatively common.

Remarks

The distance between zooids and the length of the connecting tubules, as well as the length of the pillar-like structures for adhering to the substratum, already depicted by Harmelin [14] (fig. 2.4), vary seemingly in relation to irregularities in the encrusted surface. Otherwise, morphological and morphometric differences with the type material, including the concave proximal border of the opesia and the smaller autozooidal and opesial measurements in the single colony described by Canu & Bassler [25] from Tunisia, that only included the ancestrula and some periancestrular autozooids, could express ontogenetic intraspecific variability.

Distribution

Bryobifallax disjuncta comb. nov. seems to be endemic to the Mediterranean Sea. It was described from Tunisian waters, from calcareous concretions associated with material collected by sponge fishers [25]. Further records are occasional and consistently restricted to the eastern sector of the Mediterranean Sea (i.e., Aegean Sea: [17]). In addition to the material from Lesvos Island, colonies of *B. disjuncta* comb. nov. were also reported from several localities around Chios Island (Cape Masticho: 40–60 m, Venetiko: 15 m, Dhiaporia: 50 m; Kokkina, Emborios bay: 3–15 m) by Hayward [15]. Harmelin [14] found the species on biogenic concretions collected in the southernmost Aegean localities in the Karpathos Strait (60 m) and near Santorini (110–128 m). The species is also known from Lebanon, reported off Tripoli by Harmelin et al. [18].

3.3. Family Caleschariidae Cook & Bock, 2001 [62]

Genus *Tretosina* Canu & Bassler, 1927.
Type species *Floridinella arcifera* Canu & Bassler, 1927.

3.3.1. *Tretosina arculifera* (Canu & Bassler, 1927) comb. nov.
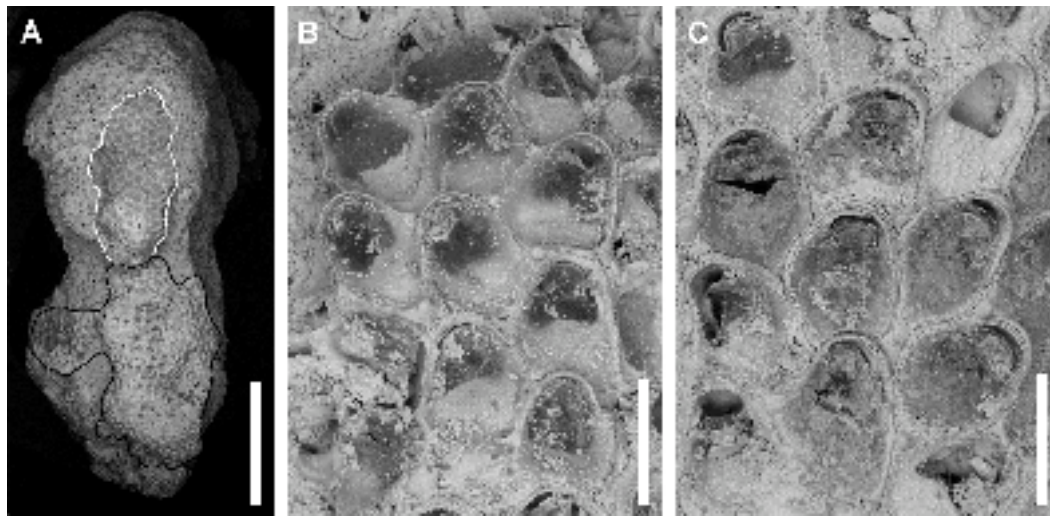
(Figures 9 and 10, Table 3)

Figure 9. *Tretosina arculifera* (Canu & Bassler, 1927). Unbleached colony from the walls of Fara cave. PMC Rosso-Collection GR. H. B.83a-1. Sample F4A. (**A**) Multilayered colony (outlined in black) increasing the diameter of a donut-shaped nodule (upper side on the right) growing along its edge together with other species including *O. vibraculifera* (outlined in white). (Scale bar: 5 mm). (**B**) Marginal autozooids of a growing lobe. (Scale bar: 500 μm). (**C**) Group of autozooids from an old part of the colony, some showing multiple intramural regenerations. (Scale bar: 500 μm).

Synonymies

Floridinella arculifera Canu & Bassler 1927 [63] (p. 7, pl. 2, fig. 1).
Floridinella arculifera (=*Caleschara minuta*) Cook & Bock 2001 [62] (fig. 16).
non *Caleshara minuta* Cook & Bock 2001 [62] (fig. 15).
Onychocellidae sp. 1, Rosso et al. 2019a [4] (tab. 1); Rosso et al. 2019 [5] (fig. 1B, tab. 1).

Material Examined

Three living and two dead colonies on nodular concretions, including ovicellate zooids. Aegean Sea, Lesvos Island, Fara cave, sampling station F4, ca. 17 m depth, between 30 and 40 m from the entrance, dark cave walls dominated by serpulids and sponges; Agios Vasilios cave, sampling station VC2, ceiling at the dark cave sector, between 15 and 25 m from the entrance, one dead colony. Deposited under the collective code PMC Rosso-Collection GR. H. B.83a.

Description

Colony encrusting, unilaminar (Figures 9A and 10A), with the ancestrular zone located at the periphery; fan-shaped becoming somewhat lobate with evidence of lateral regenerations (Figure 11 A), junctions and possible fusions of lobes in larger colonies (about 2 cm^2) and self-overgrowth on senescent-dead zooids.

Autozooids quincuncially arranged (Figure 9B,C, Figures 10B and 11A), thick and large (mean ± SD: 648 ± 70 × 418 ± 45 μm), distinct by narrow and deep furrows; irregularly polygonal proximally, arched distally (Figures 10 and 11A), communicating through a row of septular pores in the vertical walls (Figure 10F). Marginal rim raised, mostly distally, regularly and finely beaded. Gymnocyst extremely narrow, only visible along zooidal boundaries and slightly more at proximal corners, occasionally forming low elevations (Figure 9B). Cryptocyst extensive, depressed, steeply sloping from the margins, generally flat but sometimes swollen centrally and proximally to the opesia; flanking the opesia,

tapering laterally, absent distally (Figure 10C–E and Figure 11A,B); granular with, variably sized, sparse and randomly distributed granules, which become finer and more closely packed if an ovicell is present. Distal margin straight or slightly convex medially, and then flanked by two, usually shallow, opesiular indentations.
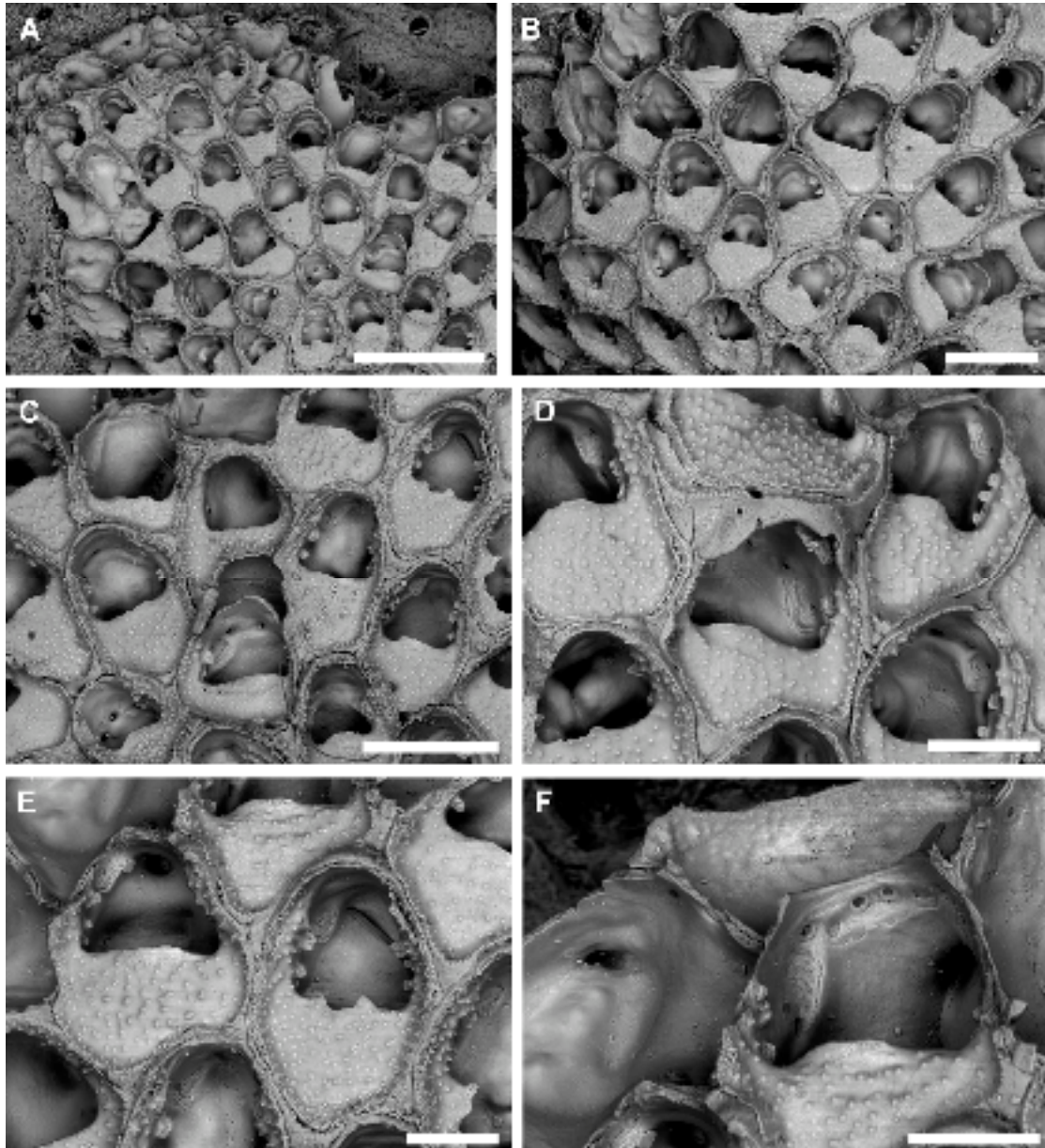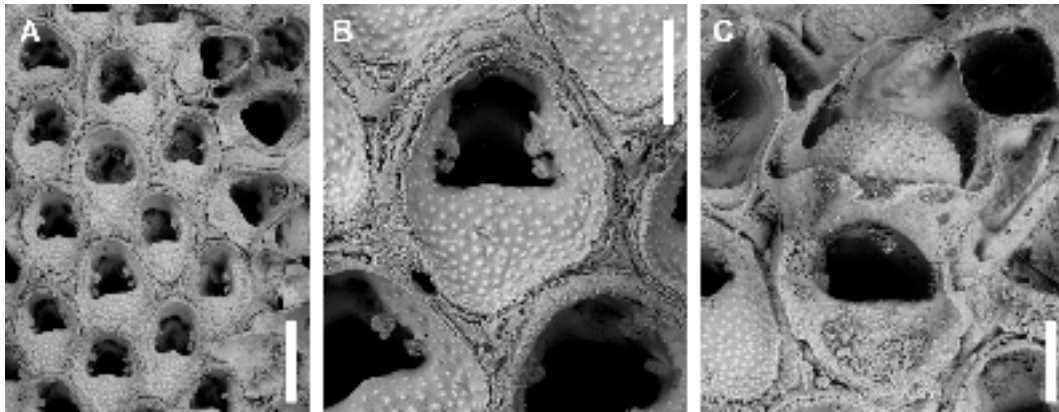

Figure 10. *Tretosina arculifera* (Canu & Bassler, 1927). Bleached colony from the walls of Fara cave. PMC Rosso-Collection GR. H. B.83a-2. Sample F4A. (**A**) General appearance of a colony lobe. (Scale bar: 1 mm). (**B**) Autozooids. (Scale bar: 500 µm). (**C**) Group of zooids, one with a broken ooecium. (Scale bar: 500 µm). (**D**) Slightly inclined, ovicellate autozooid showing the prominence of the ooecium with a transverse gymnocystal proximal rim narrowing in the centre. Some zooids show signs of intramural budding, including a greater number of lateral processes placed at different heights in the opesia. (Scale bar: 250 µm). (**E**) Autozooids, one with denticles on the proximal margin of the opesia. (Scale bar: 200 µm). (**F**) Inclined view of incomplete zooids showing uniporous septula along the walls and muscle scars. (Scale bar: 200 µm).

Figure 11. *Tretosina arculifera* (Canu & Bassler, 1927). Bleached colony from the walls of Fara cave. PMC Rosso-Collection GR. H. B.83a-3. Sample F4A. (**A**) Group of autozooids. Note the multiple regeneration characterising the colony on the right side. (Scale bar: 500 μm). (**B**) Close-up of an autozooid with multiple intramural budding. The two proximal processes are placed in a lower position than usual. (Scale bar: 200 μm). (**C**) Incomplete ooecium with missing distal autozooidal calcification. (Scale bar: 200 μm).

Opesia large, occupying about half of the frontal surface, semielliptical to subtrapezoidal with blunt corners (Figure 10A–E and Figure 11A), longer than wide (mean ± SD: 282 ± 31 × 263 ± 30 μm). One to three large processes protruding from each side at opesia mid-length (but proximally to the operculum), at the same level as the lateral cryptocyst or more deeply inside the opesia (Figure 10C,D); usually quadrangular with the flat, frontally-facing surface irregularly to concentrically laminated and etched (Figure 11C). Occasionally, one or two denticles occur on the distal cryptocystal margin (Figure 10E). Muscle scars irregularly elliptical, longitudinally elongate or quadrangular, visible very distally through the opesia (located nearly at opercular level) on projections of the lateral walls (Figure 10D,F). Spines absent. Operculum small, corresponding usually to less than half the length and width of the opesia (Figure 9B,C).

Ovicell endozooidal, globose but not prominent (Figure 10D), fully immersed in the thickness of the distal autozooid, formed by a folding of the distal autozooid, lining its frontal surface but leaving a narrow space below its floor, protruding for about the entire cryptocystal length (Figure 11C); outer surface mostly cryptocystal (and covered by the frontal membrane in living colonies), produced by the distal autozooid and showing a feebly raising, more finely and densely granular cryptocyst than other autozooids; proximal border slightly raised and thickened formed by a markedly developed gymnocystal band. Operculum of the maternal zooid apparently not dimorphic.

Avicularia absent. Ancestrula not observed; putative periancestrular zooids arranged in a three-row divergent fan.

Remarks

Our specimens fit well in *Floridinella arculifera*, as described and figured by Canu & Bassler [63] from Hawaii, although the opesia of the Pacific specimens tends to be more trifoliate, with the proximal border more convex distally and two deeper opesiular indentations than in the Mediterranean colonies. However, *Floridinella* Canu & Bassler, 1917 (type species *F. vicksburgica* Canu & Bassler, 1917 from the Oligocene of Alabama, USA) has avicularia, which are missing in this species. Avicularia of *F. vicksburgica* were observed by Cook & Bock [62] and described as small with triangular rostra and complete crossbar, transversely oriented on ovicells. Furthermore, ovicells are subimmersed in this species, although described [64,65] and sometimes reported (e.g., [66]) as endozooidal.

Based on its endozooidal ovicell and the absence of avicularia, *Floridinella arculifera* has been placed in *Caleschara* MacGillivray, 1880 by Cook & Bock [62]. These authors contextually synonymized it with *Caleschara minuta* (Maplestone, 1909), a species from the Gilbert Islands and with two further

Indo-Pacific species, i.e., *C. levinseni* Harmer, 1926 from the Kei Islands (Moluccas) and *C. laxa* Canu & Bassler, 1929 from the Philippines. After a careful re-examination of the illustrations and descriptions provided by Cook & Bock [62], as well as Tilbrook [67] (*C. minuta*), and Gordon [68], who suggested the conspecificity of *Caleschara levinseni* and *C. laxa*, we agree to retain the synonymy of *Caleschara minuta* with *C. levinseni* and *C. laxa* but we suggest to reconsider *Floridinella arculifera* as a separate species. Indeed, the specimen figured by Cook & Bock [62] (fig. 16) lacks the median cryptocystal denticle that is constantly prominent in *C. minuta* [62] (fig. 15) and, hence, the lateral cryptocystal indentations producing the typical trifoliate opesia. Cryptocystal denticles protruding all along the lateral sides of the opesia are wide in *C. minuta* but decidedly less developed in *F. arculifera* from Hawaii and in our specimens from Lesvos. Furthermore, only occasionally denticles have been found at the level with the cryptocyst, whereas they mostly protrude from lateral walls at different heights and all show a flat, frontally-facing surface (see description and morphofunctional comments below). Finally, the cryptocyst is only slightly depressed in relation to the mural rim, and its granules are finer and more densely packed than in *C. minuta*.

The generic allocation of *F. arculifera* is challenging. The species shares several characters with both *Caleschara* and *Tretosina* Canu & Bassler, 1927 of the family Calescharidae Cook & Book, 2001. Focusing on the external morphology, the absence of a median denticle questions the placement in *Caleschara* although the oldest representative of *Caleschara* known to date, from the early Eocene of the Chatham Islands, lacks a median cryptocystal denticle [69]. However, the median cryptocystal denticle typically occurs in species of *Caleschara*, sometimes forming an extensive shelf leaving only a small, semielliptical opesia with long, denticulate opesiular indentations, as in the genotype *C. denticulata* (MacGillivray, 1869) (see [62]). Cryptocystal median denticles are missing in two species of *Tretosina* (i.e., *T. moderna* Cook, 1985 from present-day West Africa, and *T. flemingi* (Brown, 1952) from the Pliocene of New Zealand), but in the type species *T. arcifera* Canu & Bassler, 1927 from the Miocene of Victoria (Australia) it is inconstant and very small. Furthermore, both genera possess a vertical lamina descending from the cryptocyst and separating the internal autozooidal space in two compartments (see [62]) (figs 22, 24). This lamina is absent in the Lesvos specimens as it is in *T. moderna* and *T. flemingi*. For all the above reasons, we suggest the new combination *Tretosina arculifera* comb. nov.

This is the first record of the genus *Tretosina* and the family Calescharidae from the Mediterranean and European waters. Only a fossil Danian to Montian species, *Caleschara squamosa* (Meunier & Pergens, 1886), has been reported from Belgium [70], but this fossil species (only known from the type material) has much smaller autozooids (400×200 μm) with distinctive scales on the cryptocyst, a well-developed median process and narrow elongated opesiular indentations (Voigt 1987, fide [62]).

We interpreted the structures protruding from the lateral walls and having a flat roughly annulated upward-facing surface, as possible bases for the attachment of muscles. Similar structures are present in *T. arcifera* [62] (fig. 24) and in the autozooids of *Parastichopora vanna* Cook & Chimonides, 1981, for which the authors hypothesised the same function [71].

Distribution

This is the first record of *T. arculifera* comb. nov. after its original description by Canu & Bassler [63]. The original finding is dated July 1902; a few colonies, some of which alive and fertile, were collected at the depth range of 91–113 m off Hawaii and 142–406 m off Molokai Island, in coral habitats at 20.6 °C. Subsequent citations, including Winston [72] (p. 7), Tilbrook [67] (p. 72, 73) and Cook & Bock [62] (p. 536, fig. 16), always refer to these same colonies. No obvious morphological differences distinguish our specimens from those figured from Hawaii in addition to the variability of the opesia shape (see Remarks). For this reason, we refrain from introducing a new species. While similarities between deep shelf to upper bathyal habitats and shallow-water caves [28,73,74] may explain the difference in depths between these two records, the great geographical distance is puzzling. More data and possibly phylogenetic analysis are needed either to support the possible transport and introduction of this rare species into the Mediterranean Sea or to reveal a species complex.

4. Discussion

Examination of the bryozoan component from two submarine caves of Lesvos Island, NE Aegean Sea, confirmed the occurrence of two out of the three species of *Onychocella* known to date from this basin, i.e., *O. marioni* and *O. vibraculifera*. The urge for a revision of the type material of both *O. marioni* and *O. angulosa* (the third Mediterranean species) to ascertain their conspecificity is remarked once more because necessary to clarify the diversity and distribution of this genus in the Mediterranean, as well as in the near Atlantic from where both species have been reported [13,29]. The proposed new combination, *Bryobifallax disjuncta* comb. nov., and the placement of this species in Microporidae further decreases the number of species and genera of Mediterranean onychocellids.

It is worth noting that, with the exception of *O. marioni,* all these species are restricted to the Mediterranean Sea. *Onychocella vibraculifera* and *B. disjuncta* comb. nov. are endemic and restricted to the eastern sector of the basin with the exception of the first described colony [25].

Onychocella is a long-living genus with several species known from the Mediterranean area and European regions since the Cretaceous [57], but a reliable stratigraphic distribution of the species here treated, possibly going back to the late Miocene and the Pleistocene for *O. marioni* and *O. vibraculifera* respectively, remains to be established (see Remarks for each of these species and [29]).

Tretosina arculifera comb. nov. increases to four the number of species now assigned to this genus, which also includes the Miocene *T. arcifera* from Australia, the Pliocene *T. flemingi* [75] from New Zealand, and the Recent *T. moderna* Cook, 1985 from west Africa [33]. The inclusion of *Tretosina arculifera* comb. nov. within *Tretosina* and its finding in the eastern Mediterranean after its historical record from Hawaii [63], widen the present-day geographical distribution of this genus previously only reported from west Africa [34]. The record of this species and genus in the Mediterranean also widens the geographical distribution of Calescharidae previously restricted to the Atlantic (*T. moderna*) and the Indo-Pacific. However, because information on these taxa is still too fragmentary, any biogeographical hypothesis would be speculative.

A morphological/developmental feature common to all the species/specimens described here is the presence of successive intramural buds affecting both autozooids and vicarious avicularia. Subsequent intramural buds were interpreted either as evidence for high predation pressure [76] or as an effect of the ageing process [6,77]. In submarine cave habitats like those studied here, the recycling of existing modules seems to be linked to changes in nutrient availability, with induced senescence during phases of lower nutrient levels alternating with intramural budding during phases of higher nutrient levels [6,76].

References

1. Imperato, F. *Historia Naturale*; Presso Combi, & la Noù: Venetia, Italy, 1599.

2.   Coll, M.; Piroddi, C.; Steenbeek, J.; Kaschner, K.; Lasram, B.R.F.; Aguzzi, J.; Ballesteros, E.; Bianchi, C.N.; Corbera, J.; Dailianis, T.; et al. The biodiversity of the Mediterranean Sea: Estimates, patterns, and threats. *PLoS ONE* **2010**, *5*, e11842. [CrossRef] [PubMed]

3.   Rosso, A.; Di Martino, E. Bryozoan diversity in the Mediterranean Sea: An up-date. *Med. Mar. Sci.* **2016**, *17*, 567–607. [CrossRef]

4.   Rosso, A.; Gerovasileiou, V.; Sanfilippo, R.; Guido, A. Bryozoans assemblages from two submarine caves in the Aegean Sea (Eastern Mediterranean). *Mar. Biodivers.* **2019**, *49*, 707–726. [CrossRef]

5.   Rosso, A.; Gerovasileiou, V.; Sanfilippo, R.; Guido, A. Undisclosed bryodiversity of submarine caves of the Aegean Sea (Eastern Mediterranean). In Proceedings of the 2nd Mediterranean Symposium on the Conservation of Dark Habitats, Antalya, Turkey, 16 January 2019; RAC/SPA: Antalya, Turkey, 2019; pp. 47–52.

6.   Rosso, A.; Di Martino, E.; Gerovasileiou, V. Revision of the genus *Setosella* (Bryozoa: Cheilostomata) with description of new species from deep-waters and submarine caves of the Mediterranean. *Zootaxa* **2020**, *4728*, 401–442. [CrossRef] [PubMed]

7.   Schwaha, T.; Bernhard, J.M.; Edgcomb, V.P.; Todaro, M.A. *Aethozooides uraniae*, a new deep-sea genus and species of solitary bryozoan from the Mediterranean Sea, with a revision of the Aethozoidae. *Mar. Biodiv.* **2019**, *49*, 1843–1856. [CrossRef]

8.   Achilleos, K.; Jimenez, C.; Berning, B.; Petrou, A. Bryozoan diversity of Cyprus (eastern Mediterranean Sea): First results from census surveys (2011–2018). *Med. Mar. Sci.* **2020**, *21*, 228–237. [CrossRef]

9.   Jullien, J. Note sur une nouvelle division des Bryozoaires Cheilostomiens. *Bull. Soc. Zool. Fr.* **1882**, *6*, 271–285.

10.   Taylor, P.D.; Martha, S.O.; Gordon, D.P. Synopsis of 'onychocellid' cheilostome bryozoan genera. *J. Nat. Hist.* **2018**, *52*, 1657–1721. [CrossRef]

11.   Gautier, Y.V. Recherches écologiques sur les Bryozoaires Chilostomes en Méditerranée occidentale. *Rec. Trav. Stat. Mar. Endoume* **1962**, *38*, 1–434.

12.   Prenant, M.; Bobin, G. *Bryozoaires, deuxieme partie. Chilostomes Anasca*; Fédération Française des sociétés de sciences naturelles: Paris, France, 1966; pp. 1–647.

13.   Zabala, M.; Maluquer, P. Illustrated keys for the classification of Mediterranean Bryozoa. *Treb. Mus, Zool. Barcelona* **1988**, *4*, 1–294.

14.   Harmelin, J.-G. Bryozoaires récoltés au cours de la campagne du Jean Charcot en Méditerranée orientale (Août-Septembre 1967). I. Dragages. *Bull. Mus. nat. Hist. nat. Sér. 2* **1969**, *40*, 1179–1208.

15.   Hayward, P.J. Studies on the cheilostome bryozoan fauna of the Aegean island of Chios. *J. Nat. Hist.* **1974**, *8*, 369–402. [CrossRef]

16.   Chimenz-Gusso, C.; Nicoletti, L.; Bondanese, C. Briozoi. *Biol. Mar. Medit.* **2014**, *20* (Suppl. 1), 1–336.

17.   Gerovasileiou, V.; Rosso, A. Marine bryozoa of Greece: An annotated checklist. *Biodiv. Data J.* **2016**, *4*, e10672. [CrossRef]

18.   Harmelin, J.-G.; Bitar, G.; Zibrowius, H. High xenodiversity versus low native diversity in the south-eastern Mediterranean: Bryozoans from the coastal zone of Lebanon. *Med. Mar. Sci.* **2016**, *17*, 417–439. [CrossRef]

19.   Gerovasileiou, V.; Trygonis, V.; Sini, M.; Koutsoubas, D.; Voultsiadou, E. Three-dimensional mapping of marine caves using a handheld echosounder. *Mar. Ecol. Prog. Ser.* **2013**, *486*, 13–22. [CrossRef]

20.   Gerovasileiou, V.; Voultsiadou, E. Sponge diversity gradients in marine caves of the eastern Mediterranean. *J. Mar. Biol. Assoc. UK* **2016**, *96*, 407–416. [CrossRef]

21.   Gerovasileiou, V.; Dimitriadis, C.; Arvanitidis, C.; Voultsiadou, E. Taxonomic and functional surrogates of sessile benthic diversity in Mediterranean marine caves. *PLoS ONE* **2017**, *12*, e0183707. [CrossRef]

22.   Sanfilippo, R.; Rosso, A.; Guido, A.; Gerovasileiou, V. Serpulid communities from two marine caves in the Aegean Sea, eastern Mediterranean. *J. Mar. Biol. Assoc. UK* **2017**, *97*, 1059–1068. [CrossRef]

23.   Rosso, A.; Di Martino, E.; Sanfilippo, R.; Di Martino, V. Bryozoan communities and thanatocoenoses from submarine caves in the plemmirio marine protected area (SE Sicily). In *Bryozoan Studies 2010, Proceedings of the 15th IBA Conference, Kiel, Germany, 16−18 May 2010*; Ernst, A., Schäfer, P., Scholz, J., Eds.; Lecture Notes in Earth System Sciences; Springer: Berlin/Heidelberg, Germany, 2013; Volume 143, pp. 251–269.

24.   Canu, F. Révision des Bryozoaires du Crétacé figurés par d'Orbigny. II, Cheilostomata. *Bull. Soc. Géol. Fr.* **1900**, *28*, 334–463.

25.   Canu, F.; Bassler, R.S. Bryozoaires marins de Tunisie. *Ann. Stat. Océanogr. Salammbô.* **1930**, *5*, 1–91.

26. Rosso, A. Popolamenti e tanatocenosi a Briozoi di fondi mobili circalitorali del Golfo di Noto (Sicilia SE). *Nat. Sicil.* **1996**, *20*, 189–225.

27. Di Geronimo, I.; Di Geronimo, R.; Improta, S.; Rosso, A.; Sanfilippo, R. Preliminary observation on a columnar coralline build-up from off SE Sicily. *Biol. Mar. Medit.* **2001**, *8*, 229–237.

28. Rosso, A.; Sanfilippo, R.; Taddei Ruggiero, E.; Di Martino, E. Faunas and ecological groups of Serpuloidea, Bryozoa and Brachiopoda from submarine caves in Sicily (Mediterranean Sea). *Boll. Soc. Paleont. Ital.* **2013**, *52*, 167–176.

29. Berning, B. The cheilostome bryozoan fauna from the Late Miocene of Niebla (Guadalquivir Basin, SW Spain): Environmental and biogeographic implications. *Mitt. Geol. Paläont. Inst. Univ. Hambg.* **2006**, *90*, 7–156.

30. Unsal, I. Bryozaires marins de Turquie. *Istambul Üniv. Fen Fakül Mecmuasi Ser. B* **1975**, *40*, 37–54.

31. Reuss, A.E. Die fossilen Polyparien des Wiener Tertiärbeckens. *Haid. Naturwis. Abhand.* **1848**, *2*, 1–109.

32. Zágoršek, K. Bryozoa from the Langhian (Miocene) of the Czech Republic. Part I: Geology of the studied sections, systematic description of the orders Cyclostomata, Ctenostomata and "Anascan" Cheilostomata (Suborders Malacostega Levinsen, 1902 and Flustrina Smitt, 1868). *Acta Mus. Nat. Prague Ser. B Hist. Nat.* **2010**, *66*, 3–136.

33. Cook, P.L. Polyzoa from West Africa. 1. Notes on the Steganoporellidae, Thalamoporellidae, and Onychocellidae. *Result. Sci. Camp. Calypso* **1964**, *41*, 43–78.

34. Cook, P.L. Bryozoa from Ghana: A preliminary survey. *Ann. Mus. Afr. Cent. Sci. Zool.* **1985**, *238*, 1–315.

35. Gautier, Y.V. Résultats scientifiques des campagnes de la Calypso. *Ann. Inst. Oceanogr.* **1956**, *32*, 189–225.

36. Zabala, M. Fauna dels Briozous dels Països Catalans. *Inst. Est. Catalans Arx. Sec. Ciénc. Barc.* **1986**, *84*, 1–836.

37. Harmelin, J.-G. Bryozoan-dominated assemblages in Mediterranean cryptic environments. In *Bryozoa: Ordovician to Recent*; Nielsen, C., Larwood, G.P., Eds.; Olsen & Olsen: Fredensborg, Denmark, 1985; pp. 135–143.

38. WoRMS Editorial Board. World Register of Marine Species. 2020. Available online: http://www.marinespecies.orgatVLIZ (accessed on 3 September 2020).

39. Rosso, A.; Sanfilippo, R. The contribution of bryozoans and serpuloideans to coralligenous concretions from SE Sicily. In Proceedings of the First Symposium on the Coralligenous and Other Calcareous Bio-concretions of the Mediterranean Sea, Tabarka, Tunisia, 15–16 January 2009; UNEP-MAP-RAC/SPA: Tabarka, Tunisia, 2009; pp. 123–128.

40. Di Geronimo, I.; Di Geronimo, R.; Rosso, A.; Sanfilippo, R. Structural and taphonomic analysis of a columnar build-up from Sicily shelf. *Géobios. Mem. Spec.* **2002**, *24*, 86–95. [CrossRef]

41. Di Geronimo, I.; Giacobbe, S.; Rosso, A.; Sanfilippo, R. Popolamenti e tanatocenosi del Banco Apollo (Ustica, Mar Tirreno meridionale). *Boll. Mus. Reg. Sc. Nat. Torino* **1990**, *spec*, 697–729.

42. Rosso, A. Valutazione della biodiversità in Mediterraneo: L'esempio dei popolamenti a briozoi della Biocenosi del Detritico Costiero. *Biol. Mar. Medit.* **1996**, *3*, 58–65.

43. Balduzzi, A.; Rosso, A. Briozoi. In *Grotte Marine: Cinquant'anni di Ricerca in Italia*; Cicogna, F., Bianchi, N.C., Ferrari, G., Forti, P., Eds.; CLEM-ONLUS, Ministero dell'Ambiente e della Tutela del Territorio: Massa Lubrense, Napoli, Italy, 2003; pp. 195–202.

44. Harmelin, J.-G. Le sous-ordre des Tubuliporina (Bryozoaires Cyclostomes) en Méditerranée. Écologie et systématique. *Mém. Inst. Océanogr.* **1976**, *10*, 1–326.

45. Harmelin, J.-G. Biodiversité des habitats cryptiques marins du parc national de Port-Cros (Méditerranée, France). Assemblages de bryozoaires d'une grotte sous-marine et des faces inférieures de pierres. *Sci. Rep. Port-Cros Natl. Park Fr.* **2003**, *19*, 101–116.

46. Harmelin, J.G. Patterns in the distribution of bryozoans in the Mediterranean marine caves. *Stygologia* **1986**, *2*, 10–25.

47. Gili, J.M.; Olivella, I.; Zabala, M.; Ros, J. Primera contribución al conocimiento del poblamiento de las cuevas submarinas del litoral catalán. In *Actas del Ier Simposio Ibérico de Estudio del Bentos Marino*; Niell, F.X., Ros, J.D., Eds.; Universidad del País Vasco: Bilbao, Spain, 1982; pp. 818–836.

48. Morri, C.; Bianchi, C.N.; Cocito, S.; Peirano, A.; De Biase, A.M.; Aliani, S.; Pansini, M.; Boyer, M.; Ferdeghini, F.; Pestarino, M.; et al. Biodiversity of marine sessile epifauna at an Aegean island subject to hydrothermal activity: Milos, eastern Mediterranean Sea. *Mar. Biol.* **1999**, *135*, 729–739. [CrossRef]

49. Koçak, F.; Balduzzi, A.; Benli, H.A. Epiphytic bryozoan community of *Posidonia oceanica* (L.) Delile meadow in the northern Cyprus (Eastern Mediterranean). *Indian J. Mar. Sci.* **2002**, *31*, 235–238.

50. Koçak, F.; Aydin Önen, S. Checklist of Bryozoa on the coasts of Turkey. *Turkish J. Zool.* **2014**, *38*, 880–891. [CrossRef]

51. Neviani, A. Briozoi fossili della Farnesina e Monte Mario presso Roma. *Palaeontogr. Ital.* **1985**, *1*, 79–100.

52. Rosso, A.; Chimenz Gusso, C.; Balduzzi, A. Bryozoa. Checklist della Flora e della Fauna dei Mari Italiani (Parte II). *Biol. Mar. Medit.* **2010**, *17*, 589–615.

53. Winston, J.E.; Vieira, L.M. Systematics of intertidal incrusting bryozoans from southeastern Brazil. *Zootaxa* **2013**, *3710*, 101–146. [CrossRef] [PubMed]

54. Di Geronimo, I.; La Perna, R.; Rosso, A.; Sanfilippo, R. Popolamento e tanatocenosi bentonica della Grotta dell'Accademia (Ustica, Mar Tirreno meridionale). *Nat. Sicil.* **1993**, *17*, 45–63.

55. Di Geronimo, I.; Allegri, L.; Improta, S.; La Perna, R.; Rosso, A.; Sanfilippo, R. Spatial and Temporal aspects of Recent benthic thanatocoenoses in a Mediterranean Infralittoral cave. *Riv. It. Paleont. Strat.* **1997**, *103*, 15–28.

56. Harmer, S.F. The Polyzoa of the Siboga Expedition, 2. Cheilostomata Anasca. *Siboga Exped. Rep.* **1926**, *28*, 183–501.

57. Bock, P.E. Bryozoa Home Page. Available online: http://www.bryozoa.net (accessed on 31 August 2020).

58. Ostrovsky, A.N. Evolution of sexual reproduction in marine invertebrates. In *Example of Gymnolaemate Bryozoans*; Springer: Dordrecht, The Netherlands, 2013; pp. 1–356.

59. Hayward, P.J. *Antarctic Cheilostomatous Bryozoa*; Oxford University Press: Oxford, UK, 1995; pp. 1–355.

60. Moyano, G.H.I. *Flustrapora magellanica* nov. gen. nov. sp., (Bryozoa, Cheilostomata, Anasca). *Bol. Soc. Biol. Concepción* **1970**, *42*, 59–65.

61. Souto, J.; Reverter-Gil, O.; Ostrovsky, A.N. New species of Bryozoa from Madeira associated with rhodoliths. *Zootaxa* **2014**, *3795*, 135–151. [CrossRef]

62. Cook, P.L.; Bock, P.E. Calescharidae, a new family for the Tertiary to Recent genera *Caleschara* MacGillivray and *Tretosina* Canu & Bassler (Bryozoa: Cheilostomata). *Inv. Taxon.* **2001**, *15*, 527–550.

63. Canu, F.; Bassler, R.S. Bryozoaires des Iles Hawaii. *Bull. Soc. Sci. Seine Oise* **1927**, *7*, 1–66.

64. Canu, F.; Bassler, R.S. A synopsis of American Early Tertiary cheilostome Bryozoa. *Bull. U.S. Natl. Mus.* **1917**, *96*, 1–87. [CrossRef]

65. Canu, F.; Bassler, R.S. North American early tertiary bryozoa. *Bull. U.S. Natl. Mus.* **1920**, *106*, 1–879. [CrossRef]

66. Taylor, P.D.; McKinney, F.K. Cretaceous Bryozoa from the cCmpanian and Maastrichtian of the Atlantic and gulf coastal plains, United States. *Scr. Geol.* **2006**, *132*, 1–346.

67. Tilbrook, K.J. Cheilostomatous Bryozoa from the Solomon Islands. *Stud. Biodivers. St. Barbara Mus. Nat. Hist. Monogr. 4* **2006**, *3*, 1–386.

68. Gordon, D.P. The marine fauna of New Zealand: Bryozoa Ceilostomata from the Kermadek Ridge. *N. Zeal. Oceanogr. Inst.* **1984**, *91*, 1–198.

69. Gordon, D.P.; Taylor, P.D. Late Paleocene to earliest Eocene bryozoans from Chatham Islands, New Zealand. *Bull. Nat. Hist. Mus. Lond. (Geol.)* **1999**, *55*, 1–45.

70. Meunier, A.; Pergens, E. *Les Bryozoaires du Systéme Montien (Éocène inférieur)*; Louvain, Belgium, 1886; Volume 1, pp. 1–15. Available online: https://books.google.com.hk/books/about/Les_bryozoaires_du_syst%C3%A8me_montien_%C3%A9oc.html?id=F7e_GwAACAAJ&redir_esc=y (accessed on 3 September 2020).

71. Cook, P.L.; Chimonides, P.J. Morphology and systematics of some rooted cheilostome Bryozoa. *J. Nat. Hist.* **1981**, *15*, 97134. [CrossRef]

72. Winston, J.E. An annotate checklist of coral-associated bryozoans. *Am. Mus. Novit.* **1986**, *2859*, 1–39.

73. Harmelin, J.-G. Diversity of bryozoans in a Mediterranean sublittoral cave with bathyal-like conditions: Role of dispersal processes and local factors. *Mar. Ecol. Progr. Ser.* **1997**, *153*, 139–152. [CrossRef]

74. Harmelin, J.-G.; Vacelet, J.; Vasseur, P. Les grottes sous-marines obscures: Un milieu extrême et un remarquable biotope refuge. *Téthys* **1985**, *11*, 214–229.

75. Brown, D.A. *The Tertiary cheilostomatous Polyzoa of New Zealand*; Trustees of the British Museum (Natural History): London, UK, 1952; pp. 1–405.

76. Berning, B.; Tilbrook, K.J.; Rosso, A. Revision of the north-eastern Atlantic and Mediterranean species of the genera *Herentia* and *Therenia* (Bryozoa: Cheilostomata). *J. Nat. Hist.* **2008**, *42*, 1509–1547. [CrossRef]

77. Harmelin, J.-G.; Bishop, J.D.D.; Madurell, T.; Souto, J.; Jones, M.E.S.; Zabala, M. The genus *Collarina* (Bryozoa, Cheilostomatida) in the NE Atlantic-Mediterranean region: Unexpected diversity. New species and reappraisal of *C. balzaci* and *C. fayalensis*. *Zoosystema* **2019**, *41*, 385–418. [CrossRef]